Inhibiting eicosanoid degradation exerts antifibrotic effects in a pulmonary fibrosis mouse model and human tissue

Thomas Bärnthaler, MD, PhD,[a] Anna Theiler, PhD,[a] Diana Zabini, PhD,[b,c] Sandra Trautmann, BSc,[d] Elvira Stacher-Priehse, MD,[b] Ilse Lanz, BSc,[a] Walter Klepetko, MD,[e] Katharina Sinn, MD,[e] Holger Flick, MD,[f] Stefan Scheidl, MD,[f] Dominique Thomas, PhD,[d] Horst Olschewski, MD,[c,f] Grazyna Kwapiszewska, PhD,[b,c] Rufina Schuligoi, PhD,[a] and Akos Heinemann, MD[a] *Graz and Vienna, Austria, and Frankfurt, Germany*

GRAPHICAL ABSTRACT

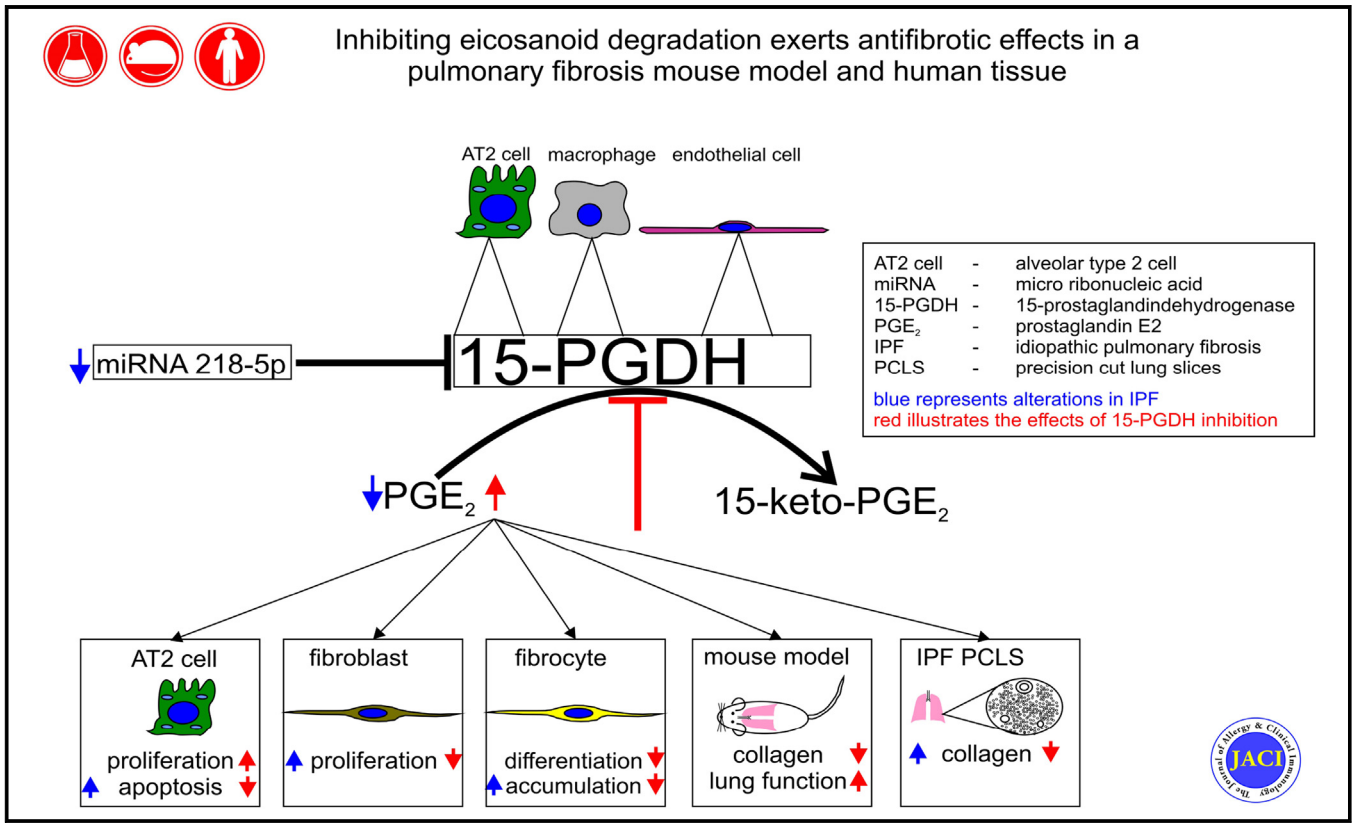

Background: Idiopathic pulmonary fibrosis (IPF) is a disease with high 5-year mortality and few therapeutic options. Prostaglandin (PG) E_2 exhibits antifibrotic properties and is reduced in bronchoalveolar lavage from patients with IPF. 15-Prostaglandin dehydrogenase (15-PGDH) is the key enzyme in PGE_2 metabolism under the control of TGF-β and microRNA 218.

From the Divisions of [a]Pharmacology and [b]Physiology, Otto Loewi Research Center, Medical University of Graz and [c]the Ludwig Boltzmann Institute for Lung Vascular Research, Graz; [d]the Pharmazentrum Frankfurt/ZAFES, Institute of Clinical Pharmacology, Goethe University Frankfurt, Frankfurt; [e]the Division of Thoracic Surgery, Department of Surgery, Medical University of Vienna, Vienna; and [f]the Department of Internal Medicine, Division of Pulmonology, Medical University of Graz, Graz.

This research was supported by the Austrian Science Fund (FWF; grant no. P22521-B18 to A.H. and grant no. P26185-B19 to R.S.), the Jubiläumsfonds of the Austrian National Bank (grant no. 14263 to A.H.), and the LOEWE program from the state of Hesse (Translational Medicine and Pharmacology, TMP, to D.T.). T.B. was funded by the PhD program DK-MOLIN (FWF–W1241) and the Start Funding Program of the Medical University of Graz. T.B. and A.T. are recipients of a doctoral fellowship of the Austrian Academy of Sciences.

Disclosure of potential conflict of interest: The authors declare that they have no relevant conflicts of interest.

Received for publication June 21, 2019; revised October 26, 2019; accepted for publication November 7, 2019.

Available online December 5, 2019.

Corresponding author: Akos Heinemann, MD, Division of Pharmacology, Otto Loewi Research Center (for Vascular Biology, Immunology and Inflammation), Medical University of Graz, Universitätsplatz 4, Graz 8010, Austria. E-mail: akos.heinemann@medunigraz.at.

The CrossMark symbol notifies online readers when updates have been made to the article such as errata or minor corrections

0091-6749

https://doi.org/10.1016/j.jaci.2019.11.032

Objective: We sought to investigate the expression of 15-PGDH in IPF and the therapeutic potential of a specific inhibitor of this enzyme in a mouse model and human tissue.

Methods: *In vitro* studies, including fibrocyte differentiation, regulation of 15-PGDH, RT-PCR, and Western blot, were performed using peripheral blood from healthy donors and patients with IPF and A549 cells. Immunohistochemistry, immunofluorescence, 15-PGDH activity assays, and *in situ* hybridization as well as *ex vivo* IPF tissue culture experiments were done using healthy donor and IPF lungs. Therapeutic effects of 15-PGDH inhibition were studied in the bleomycin mouse model of pulmonary fibrosis.

Results: We demonstrate that 15-PGDH shows areas of increased expression in patients with IPF. Inhibition of this enzyme increases PGE_2 levels and reduces collagen production in IPF precision cut lung slices and in the bleomycin model. Inhibitor-treated mice show amelioration of lung function, decreased alveolar epithelial cell apoptosis, and fibroblast proliferation. Pulmonary fibrocyte accumulation is also decreased by inhibitor treatment in mice, similar to PGE_2 that inhibits fibrocyte differentiation from blood of healthy donors and patients with IPF. Finally, microRNA 218-5p, which is downregulated in patients with IPF, suppressed 15-PGDH expression *in vivo* and *in vitro*.

Conclusions: These findings highlight the role of 15-PGDH in IPF and suggest 15-PGDH inhibition as a promising therapeutic approach. (J Allergy Clin Immunol 2020;145:818-33.)

Key words: *PGE_2, 15-PGDH, idiopathic pulmonary fibrosis, fibrocytes*

Abbreviations used

AT2 cells:	Type 2 alveolar epithelial cells
BAL:	Bronchoalveolar lavage
Col1a1:	Collagen type 1 α1
DAPI:	4′,6-Diamidino-2-phenylindole
EP receptor:	E-type prostanoid receptor
FSP:	Fibroblast specific protein
HRP:	Horseradish peroxidase
IPF:	Idiopathic pulmonary fibrosis
ISH:	*In situ* hybridization
miRNA:	MicroRNA
PCLS:	Precision cut lung slice
PG:	Prostaglandin
15-PGDH:	15-Prostaglandin dehydrogenase
pro-SPC:	Prosurfactant protein C

Idiopathic pulmonary fibrosis (IPF) is a chronic progressive disease leading to an increase in fibrotic tissue in the lung, thus reducing compliance and affecting gas exchange. This ultimately causes respiratory insufficiency and might require transplantation.[1] Otherwise, the disease is fatal, with a median survival of 3 to 4 years.[1-3] Many approaches have been taken toward possible therapies for this condition and a comprehensive review on evaluated drugs and ongoing clinical trials has recently been published.[4] So far, there are only 2 drugs for IPF treatment—the recently Food and Drug Administration–approved antifibrotic agents pirfenidone and nintedanib.[5-7] However, other targets are urgently needed, because available treatments may decelerate disease progression, but can neither halt nor cure the disease.[7]

There is strong evidence supporting the role of eicosanoids in disease models of IPF, and especially prostaglandins (PGs), with the exception of $PGF_{2\alpha}$, seem to exert beneficial effects.[8,9] Studies have shown that PGE_2 inhibits fibroblast proliferation,[10] decreases alveolar epithelial cell apoptosis,[11] is protective in bleomycin-induced pulmonary fibrosis in mice,[12,13] and inhibits myofibroblast differentiation *in vitro*.[14] The same holds true to some extent for PGD_2.[15,16] Furthermore, there are publications showing strong beneficial effects of lipoxin A4 or its more stable analogs in preventing myofibroblast formation[17] and bleomycin-induced fibrosis[18] and in improving lung function of bleomycin-treated mice.[19] Interestingly, $CD45^+$ fibrocytes, which show mesenchymal properties such as collagen type 1 or fibroblast specific protein 1 (FSP) expression,[20] have been suggested to express E-type prostanoid 2 (EP2), EP4, and I-type prostanoid receptors.[21]

It has been demonstrated that patients with IPF show significantly lower levels of PGs, particularly PGE_2, in the bronchoalveolar lavage (BAL).[22] In addition, the relation between leukotrienes and PGs is of interest, because leukotrienes are increased in IPF and seem to exert profibrotic actions.[23] Because cyclooxygenase (COX) is considered the key enzyme for PG production, there have been efforts to study whether 1 of the 2 isoenzymes, COX-1 or COX-2, is downregulated in IPF. Although there is evidence for decreased mRNA levels of COX-2, decreased PGE_2 production in fibroblasts from fibrotic lungs, and downregulation of COX-2 protein in lung parenchyma,[8,24-26] other studies found increased levels of COX-2 in fibrotic lungs, especially in the metaplastic epithelium of fibroblastic foci.[27,28] However, another study described that COX-1 is decreased in bronchial epithelium and alveolar macrophages in IPF.[29] It has been established that heterozygous COX-2–deficient mice show a stronger fibrotic response to bleomycin than do wild-type animals,[30] and COX-2 knockout mice display a more rapid decline in lung function after bleomycin treatment.[31] Remarkably, selective deletion of COX-2 in type 2 alveolar epithelial (AT2) cells did not worsen bleomycin-induced fibrosis in mice.[32] This is especially interesting, because alveolar epithelial cells rely heavily on PGE_2 to inhibit fibroblast proliferation,[10] which in turn is crucial in the development of IPF.

15-Prostaglandin dehydrogenase (PGDH) is the enzyme that is responsible for the inactivation of PGE_2, $PGF_{2\alpha}$, and other PGs, as well as lipoxin A4.[33-35] It counteracts COX by metabolizing its products. Loss-of-function mutations in humans lead to digital clubbing and primary hypertrophic osteoarthropathy.[36,37] The relatively high levels of 15-PGDH in the lung after birth are essential for decreasing circulating PGE_2, thereby facilitating the closure of the ductus arteriosus Botalli.[38] A recent study, using a novel, highly selective pharmacologic inhibitor of 15-PGDH, SW033291, found that this compound significantly increased PGE_2 contents in the mouse lung if given intraperitoneally.[39] Furthermore, 15-PGDH inhibition caused beneficial effects in a model of chronic inflammatory colitis, and accelerated liver regeneration and bone marrow reconstitution after transplantation. One of the key players in IPF, TGF-β is known to induce 15-PGDH in some cell types, including lung cancer cells.[40,41] Furthermore, a microRNA (miRNA 218a-5p) that is downregulated in IPF has been shown to control 15-PGDH expression levels.[42-44]

Therefore, we hypothesized that 15-PGDH is upregulated in the lungs of patients with IPF and decreases PGE_2 levels, thereby preventing its protective effects. In this study, we found that lungs of patients with IPF show areas of more intense 15-PGDH expression, and that inhibition of this enzyme in human IPF precision cut lung slices (PCLSs) significantly increases PGE_2 levels. Furthermore, we could show that inhibition of 15-PGDH is protective in a mouse model of bleomycin-induced pulmonary fibrosis and also decreases established fibrosis and improves lung function.

METHODS

A detailed description of ethical permits, animals, materials, and procedures is provided in the Methods section in this article's Online Repository at www.jacionline.org.

Bleomycin model

Bleomycin was given intratracheally as previously described.[45]

Real-time PCR

For relative quantification of mRNA expression, real-time PCR was performed as described previously.[46]

Immunohistochemistry/immunofluorescence

Immunostainings were performed as previously described.[46]

In situ hybridization

In situ hybridization (ISH) was performed using RNAscope kit for 15-PGDH/hydroxyprostaglandin dehydrogenase (HPGD) and BaseScope for pre-miRNA 218 (both manufactured by ACD, Newark, Calif) according to the manufacturer's protocol. For fibrocytes, chamber slides (Thermo Fisher Scientific, Waltham, Mass) were counterstained with methyl green and mounted with Histokit II (Carl Roth, Karlsruhe, Germany).

miRNA transfection

A549 cells were transfected using the Lipofectamine RNAiMAX kit (Thermo Fisher Scientific) according to the manufacturer's instructions. For *in vivo* transfection, mice were anesthetized using ketamine/xylazine as described earlier. Invivofectamine 3.0 reagent kit (Thermo Fisher Scientific) was used according to the manufacturer's instructions with some modifications.[47]

Western blot

Western blots were performed as previously described.[46]

15-PGDH activity assay

Assay and tissue preparation were performed as described previously.[48]

Precision cut lung slices

PCLSs were prepared as previously described with some modifications.[49]

Isolation and differentiation of fibrocytes

Fibrocytes were isolated and differentiated from patients with IPF and healthy donors as previously described.[50]

Data analysis

Statistical analysis was performed using GraphPad Prism 6 (GraphPad Software, Inc, San Diego, Calif). Significance was set at P less than .05. Data are given as mean ± SEM.

RESULTS

Differential expression of 15-PGDH in IPF lungs

On staining both fibrotic and healthy lungs for 15-PGDH, we could see considerable differences in the expression pattern. Although healthy lungs show a fairly even distribution of 15-PGDH (Fig 1, *A* and *B*), fibrotic areas in IPF are almost devoid of any staining, whereas intact alveolar walls show much more pronounced staining (Fig 1, *C* and *D*). However, a 15-PGDH activity assay in lung homogenates and Western blotting showed no significant differences between IPF and controls (Fig E1). ISH in the IPF lungs for 15-PGDH mRNA and immunostaining for prosurfactant protein C (pro-SPC) and vascular endothelial cadherin revealed that epithelial as well as endothelial cells express 15-PGDH (Fig 1, *F*). Furthermore, a subset of $CD68^+$ cells (eg, macrophages) expressed high levels of 15-PGDH (Fig 1, *E*). However, smooth muscle actin (Fig 1, *E*) did not and the fibroblast marker vimentin only occasionally showed colocalization with 15-PGDH (Fig E1). In healthy lungs, 15-PGDH was predominantly expressed in endothelial cells (Fig E1).

Inhibition of 15-PGDH protects mice from bleomycin-induced fibrosis

After we confirmed that 15-PGDH mRNA and activity can be observed in adult mouse lungs (Fig E2), we investigated the effects of a specific 15-PGDH inhibitor, SW033291, in a mouse model of pulmonary fibrosis. To this end, we administered bleomycin intratracheally and treated the mice with the specific 15-PGDH inhibitor twice daily, starting from day 0. In this preventive model we could show that inhibition of 15-PGDH leads to an increase in pulmonary PGE_2 levels (Fig E3). Furthermore, fibrosis as determined by histologic assessment was reduced (Fig 2, *A-D*), weight loss and mortality were decreased (Fig 2, *E* and *G*), and hydroxyproline accumulation was diminished by SW033291 as compared with vehicle treatment (Fig 2, *F*).

AT2 cell apoptosis decreases and proliferation increases in response to 15-PGDH inhibition in bleomycin-treated mice

Exaggerated apoptosis of AT2 cells has been implicated in the pathogenesis of IPF,[51] whereas PGE_2 has been shown to decrease apoptosis, and reduced PGE_2 has been associated with the apoptosis paradox in pulmonary fibrosis (ie, increased apoptosis in epithelial cells, but reduced apoptosis/increased proliferation in fibroblasts).[11] Proliferation of AT2 cells has been shown to be beneficial in the bleomycin model of lung fibrosis,[52] and PGE_2 is a potent inducer of proliferation of airway epithelial cells.[53] Therefore, we costained lung sections for pro-SPC, Ki-67, and/or cleaved caspase 3, respectively, to investigate whether 15-PGDH inhibition increased AT2 cell proliferation and counteracted bleomycin-induced apoptosis. This approach revealed a pronounced increase in apoptotic AT2 cells on bleomycin treatment as expected,[54] which was prevented by 15-PGDH inhibitor treatment (Fig 3, *A-D*). Furthermore, we found that bleomycin alone led to a slight increase in AT2 cell proliferation,[52] and this was further significantly increased by the 15-PGDH inhibitor (Fig 3, *E-H*).

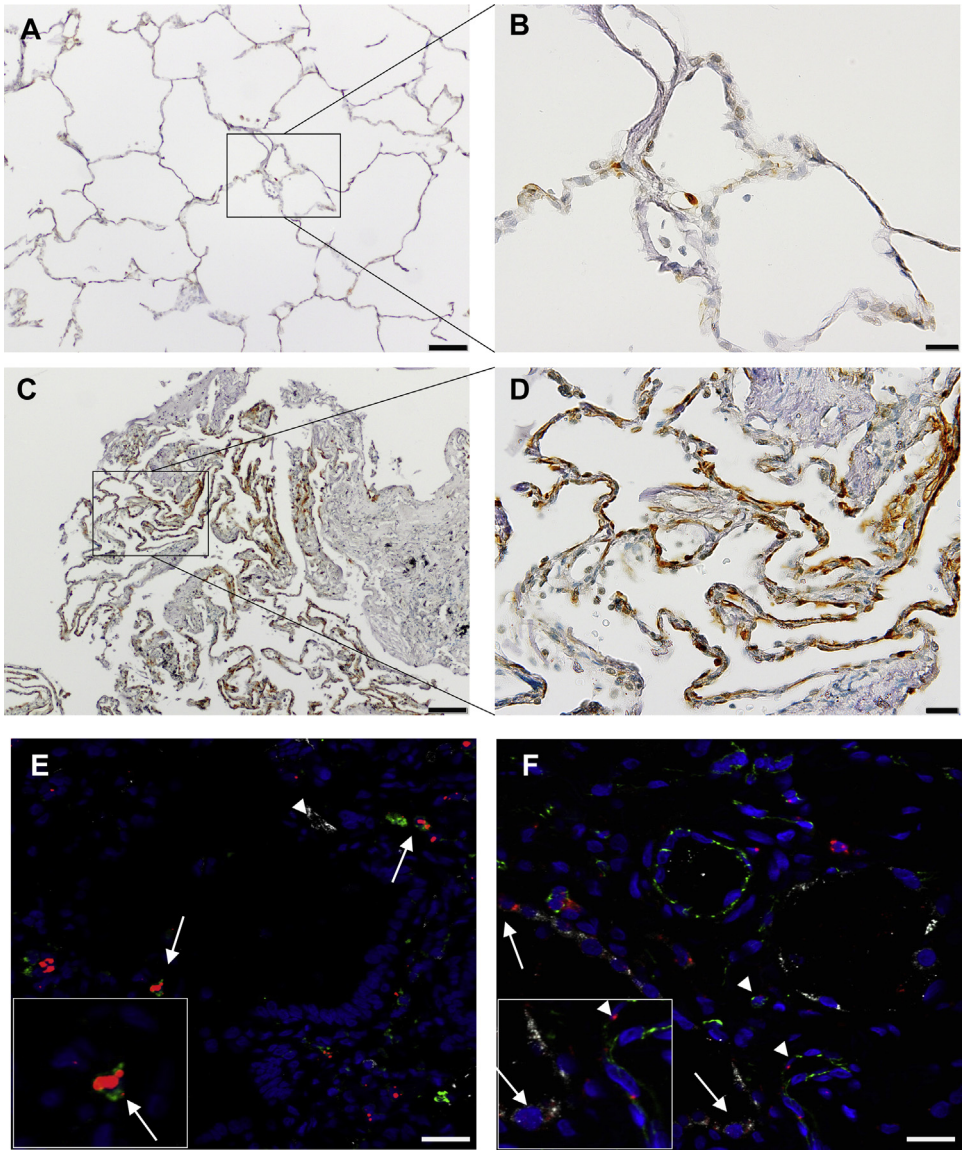

FIG 1. Expression patterns of 15-PGDH differ in healthy lungs and patients with IPF. **A-D,** Immunohistochemistry on control lung sections from organ donors and biopsy samples from patients with IPF was performed with an antibody against 15-PGDH (*brown*). Nuclei were counterstained with methyl green. Fig 1, *A* and *B,* 15-PGDH is expressed in lungs from healthy donors, mainly in the alveolar walls. *C* and *D,* Patients with IPF showed foci of more intensive staining. Images are representative for 5 controls and 5 patients with IPF. *Scale bars* indicate 200 μm (Fig 1, *A* and *C*) and 20 μm (Fig 1, *B* and *D*). ISH for 15-PGDH mRNA (*red*) and immunostaining for (**E**) CD68 (*green*) and α-SMA (*white*), or (**F**) VE-cadherin (*green*) and pro-SPC (*white*) on IPF lungs. Fig 1, *E, Arrow* shows 15-PGDH/CD68^{++} cells; *arrowhead* shows a 15-PGDH negative, α-SMA positive cell. Fig 1, *F, Arrow* shows 15-PGDH/pro-SPC double-positive cells; arrowhead shows 15-PGDH VE-cadherin double-positive cells. Images are representative for 5 patients with IPF. *E* and *F, Scale bars* indicate 20 μm; insets show double-positive cells. *α-SMA*, α-Smooth muscle actin; *VE-cadherin*, vascular endothelial cadherin.

Fibroblast proliferation is reduced on 15-PGDH inhibitor treatment in bleomycin-treated mice

Proliferation of fibroblasts has been considered a hallmark of IPF and has been shown to be increased as compared with fibroblasts from healthy controls[55] and in the bleomycin mouse model.[56] PGE_2 has been shown to suppress proliferation in lung fibroblast, which has been implicated as one of its antifibrotic pathways.[10] Thus, we set out to investigate whether this mechanism might play a role in our model. In fact, we found that bleomycin significantly increased fibroblast proliferation and this was abrogated by 15-PGDH inhibitor treatment (Fig 4, *A-D*).

Fibrocyte counts in the lungs of bleomycin-treated mice decrease in response to 15-PGDH inhibition

Fibrocytes are bone marrow–derived cells that have been shown to be increased in lungs and blood of patients with IPF

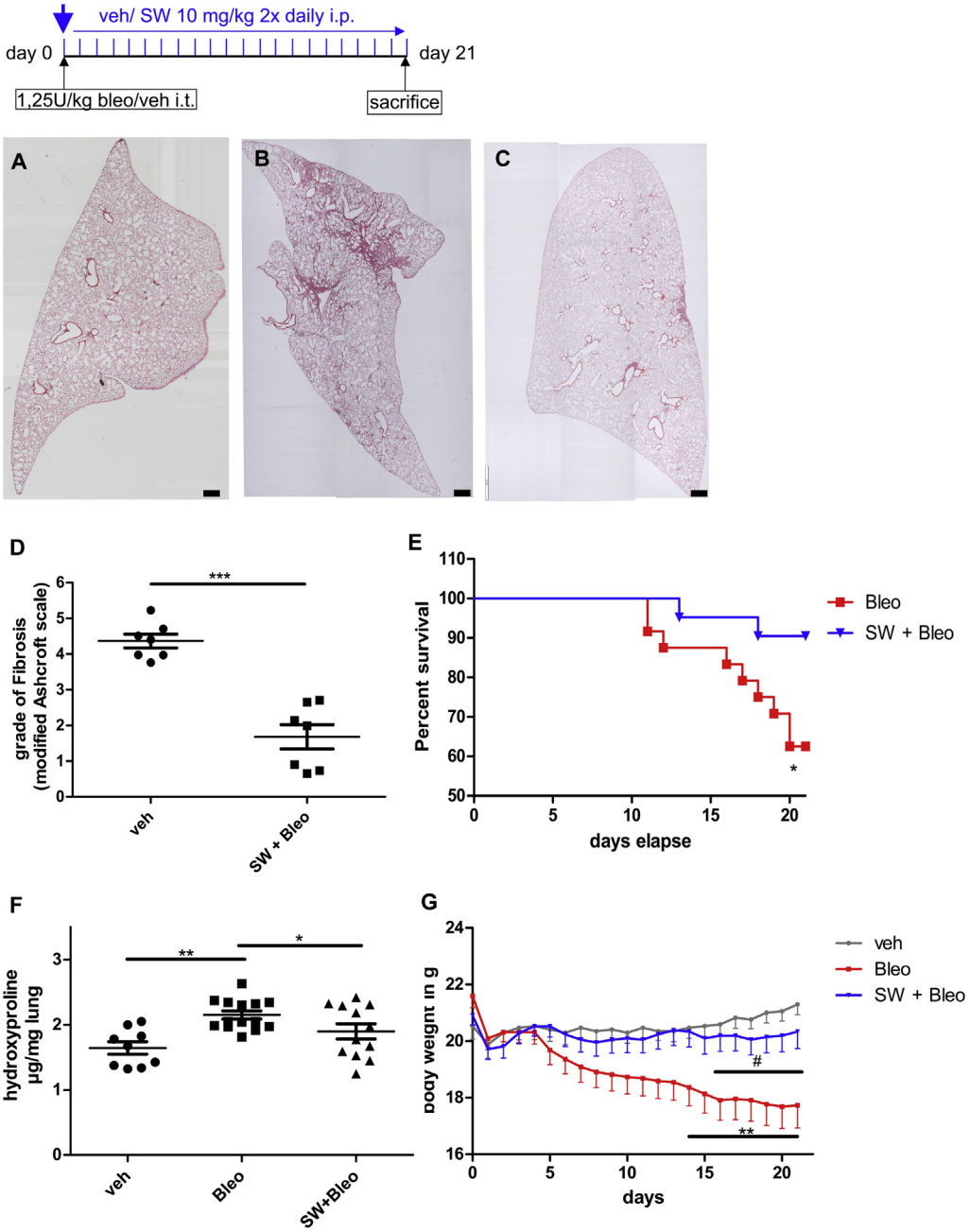

FIG 2. Inhibition of 15-PGDH ameliorates bleomycin-induced pulmonary fibrosis in a preventive model. **A-C,** Whole left lobes of mice treated with (Fig 2, *A*) vehicle (veh), (Fig 2, *B*) bleomycin (1.25 U/kg, Bleo), and (Fig 2, *C*) 15-PGDH inhibitor and bleomycin (SW + Bleo; SW033291 10 mg/kg twice daily, start on day 1) were stained with Masson's trichrome. *Scale bars* indicate 1 mm. **D,** Grade of fibrosis was determined on 60 to 70 photomicrographs of the whole lung at a 200 × magnification and scored on the basis of a modified Ashcroft scale in a double-blind fashion. **E,** Survival rate of the different treatment groups. **F,** Hydroxyproline levels, as a measurement for lung collagen, were assayed from pulverized lung homogenates. **G,** Weight was measured daily and last observation was carried forward for deceased mice. For Fig 2, *D*, Mann-Whitney *U* test was performed (n = 7-8). One-way ANOVA, followed by Newman-Keuls test, was applied in *F* (n = 8-12). For *G*, 2-way ANOVA for repeated measurements, followed by Bonferroni *post hoc* test, was applied. For *E*, Gehan-Breslow test was applied (n = 8-20). $*P < .05$, $**P < .01$, $***P < .001$; for *G*, $\#P < .05$ SW + Bleo vs Bleo.

and have been implicated to play a role in fibrotic remodeling.[20,57] Because these cells have been suggested to express EP2 and EP4 receptors, and we also noted an increase in PGE_2 in the lungs and the bone marrow (Figs E3 and E4), we were interested in knowing whether in our model fibrocyte counts in the lungs were also decreased. Double staining of lung sections with antibodies against FSP and CD45 showed that a subset of cells stains positive for both markers (representing fibrocytes[20]) in the bleomycin and

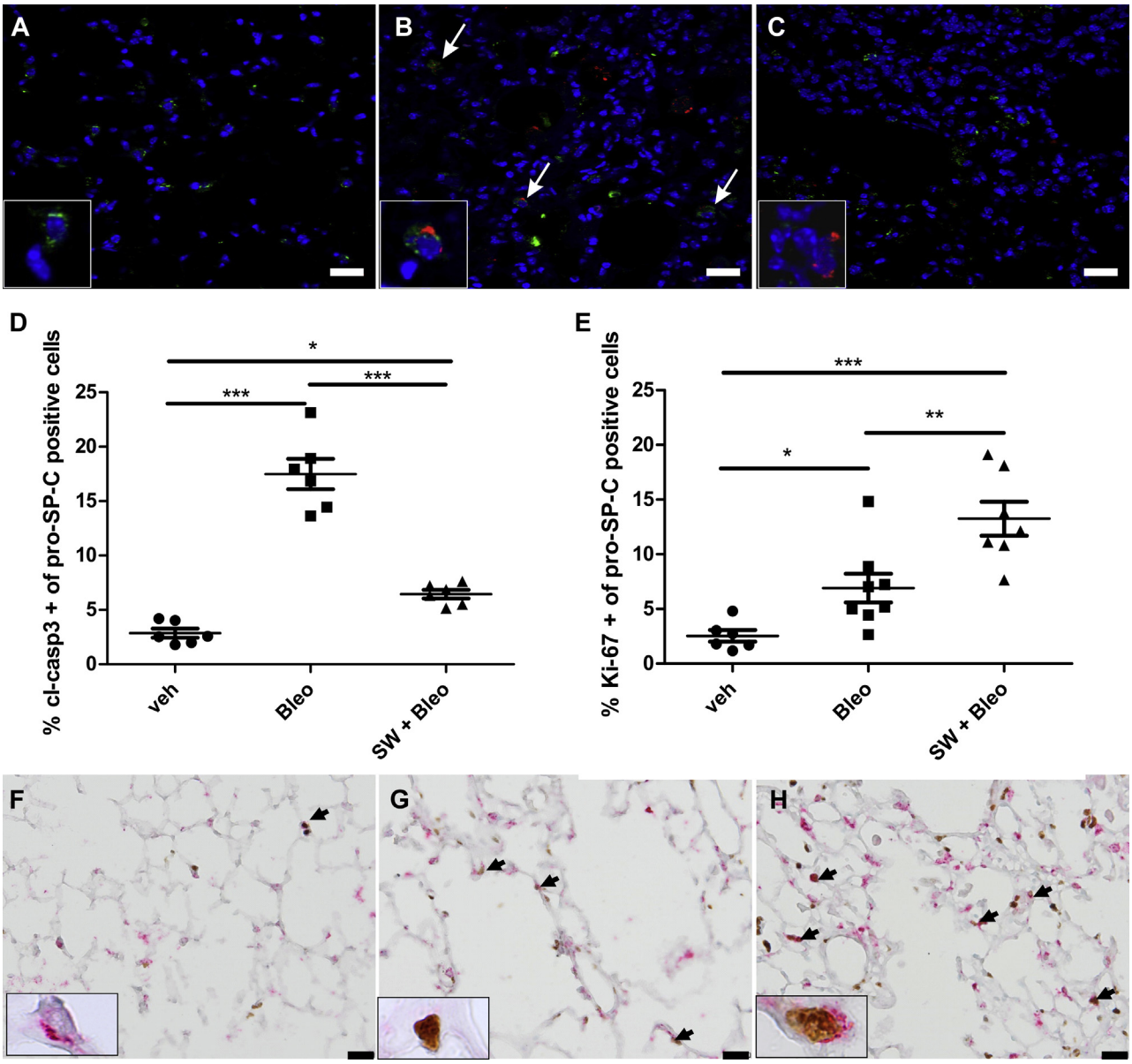

FIG 3. Inhibition of 15-PGDH reduces AT2 cell apoptosis but increases AT2 cell proliferation in the bleomycin model. **A-C**, AT2 cells (*green*) and apoptotic cells (*red*) were visualized by immunostaining sections for pro-SPC and cleaved caspase 3 (cl-casp3), respectively. Fig 3, *A*, *B*, and *C* show representative photomicrographs from vehicle (veh), bleomycin (Bleo), and bleomycin plus 15-PGDH inhibitor (SW + Bleo)–treated animals, respectively, and arrows indicate double-positive cells. Insets show (Fig 3, *A*) a cell positively stained for pro-SPC but negative for cleaved caspase 3, (Fig 3, *B*) a cell positive for both pro-SPC and cleaved caspase 3, and (Fig 3, *C*) a cell negative for pro-SPC but positive for cleaved caspase 3. **D** and **E**, Double-positive cells were counted in a double-blind fashion (in 10 hpf images per lung) and the percentage of (Fig 3, *D*) apoptotic or (Fig 3, *E*) proliferating cells of all pro-SPC positive cells was calculated. **F-H,** AT2 cells (*red*) and proliferating cells (*brown*) were visualized by immunostaining for pro-SPC and Ki-67, respectively. Fig 3, *F*, *G*, and *H* show representative photomicrographs from vehicle, bleomycin, and bleomycin plus 15-PGDH inhibitor–treated animals, respectively. *Arrows* indicate double-positive cells. Insets show (Fig 3, *F*) a pro-SPC positive/Ki-67 negative, (Fig 3, *G*) a pro-SPC negative/Ki-67 positive, and (Fig 3, *H*) a pro-SPC positive/Ki-67 positive cell. One-way ANOVA, followed by Newman-Keuls test, was applied for *D* and *E*. *Scale bars* show 20 μm. $*P < .05$, $**P < .01$, $***P < .001$.

15-PGDH inhibitor–treated group, with occasional double-positive cells also in vehicle-treated lungs (Fig 4, *F-H*). The increase in fibrocyte counts observed in the bleomycin-treated group was significantly reduced by the 15-PGDH inhibitor (Fig 4, *E-H*).

In vitro fibrocyte differentiation is inhibited by PGE_2

To investigate whether PGE_2 is able to directly target fibrocytes, we differentiated fibrocytes from PBMCs of healthy donors.[50] We found that PGE_2 treatment decreased fibrocyte differentiation in a concentration-dependent manner via EP2

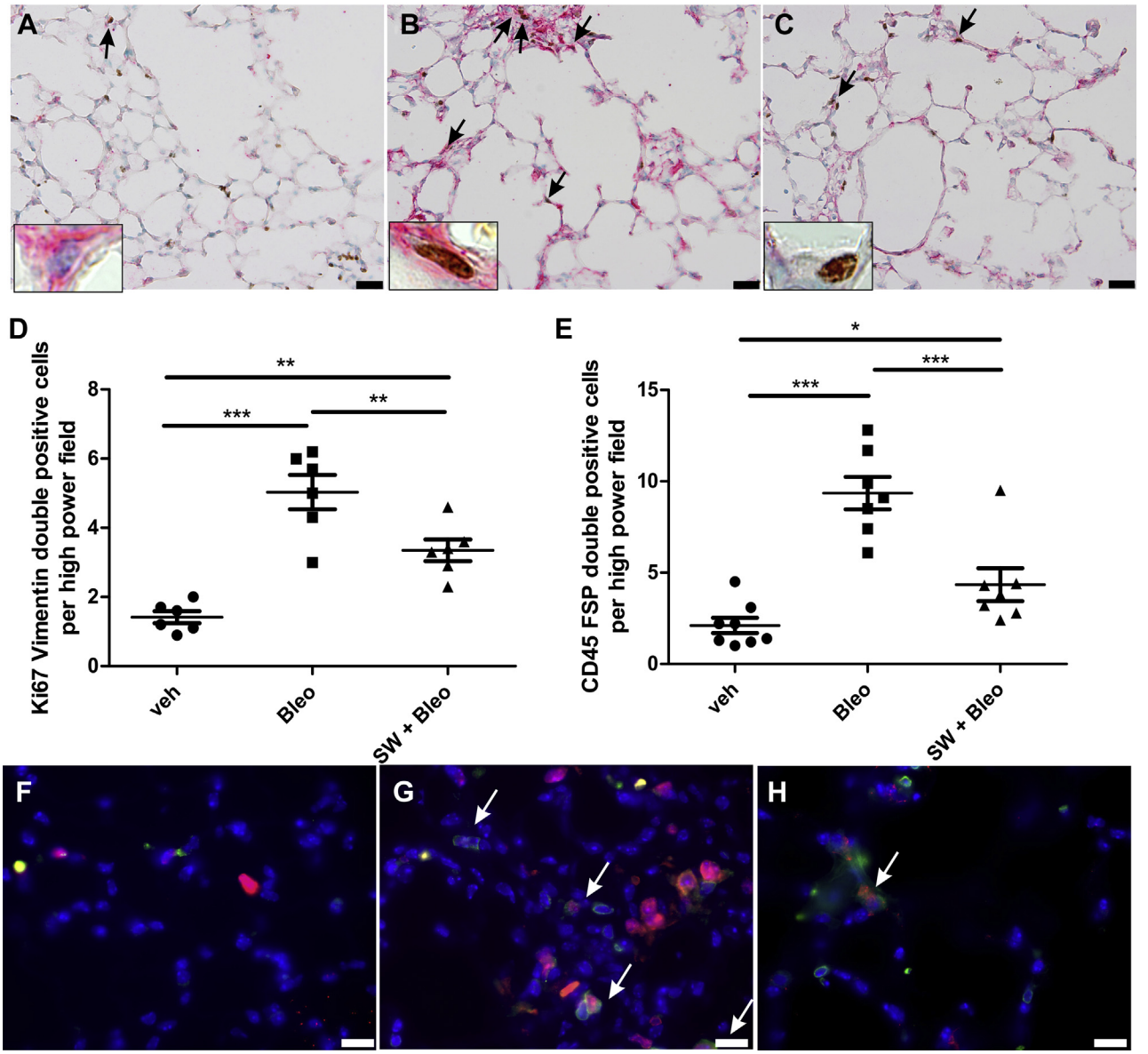

FIG 4. Inhibition of 15-PGDH reduces fibrocyte counts in the bleomycin model and decreases fibroblast proliferation. **A-C,** Fibroblasts (*red*) and proliferating cells (*brown*) were visualized by immunostaining for vimentin and Ki-67, respectively. Fig 4, *A, B,* and *C* show representative photomicrographs from vehicle, bleomycin, and bleomycin and 15-PGDH inhibitor–treated animals, respectively. *Arrows* indicate double-positive cells. Insets show (Fig 4, *A*) a vimentin-positive/Ki-67–negative cell, (Fig 4, *B*) a vimentin-positive/Ki-67–positive cell, and (Fig 4, *C*) a vimentin-negative/Ki-67–positive cell. **D** and **E,** Double-positive cells were counted in a double-blind fashion (in 10 hpf images per lung) and the number of (Fig 4, *D*) fibrocytes and (Fig 4, *E*) proliferating fibroblasts per hpf is shown. **F-H,** Fibrocytes were visualized by immunostaining sections for CD45 (*green*) and FSP (*red*). Fig 4, *F, G,* and *H* show representative photomicrographs from vehicle (veh), bleomycin (Bleo), and bleomycin plus 15-PGDH inhibitor (SW + Bleo)–treated animals, respectively. *Arrows* indicate double-positive cells. One-way ANOVA, followed by Newman-Keuls test, was applied for *D* and *E*. *Scale bars* show 20 μm. **P* < .05, ***P* < .01, ****P* < .001.

and EP4 receptor activation (Fig 5, *B* and *D*). Because it has been shown that especially EP2 receptor signaling might be impaired in IPF and the bleomycin model of pulmonary fibrosis,[58,59] we also differentiated fibrocytes from patients with IPF and found that PGE_2 exerts the same effects (Fig 5, *C*). ISH revealed abundant expression of the EP2 and EP4 receptor mRNA in both patient-derived and healthy donor–derived fibrocytes, but no expression of 15-PGDH mRNA could be observed (Fig 5, *E*).

Inhibition of 15-PGDH improves established fibrosis in the bleomycin mouse model

Because the initial phase of the bleomycin model (day 0-9) is considered to be predominantly inflammatory, we also tested the effect of 15-PGDH inhibition in the fibrotic phase, starting administration of SW033291 on day 11, consistent with a "therapeutic" approach.[60,61] Histologic assessment of the lungs showed a decrease in fibrosis grades in the inhibitor-treated group

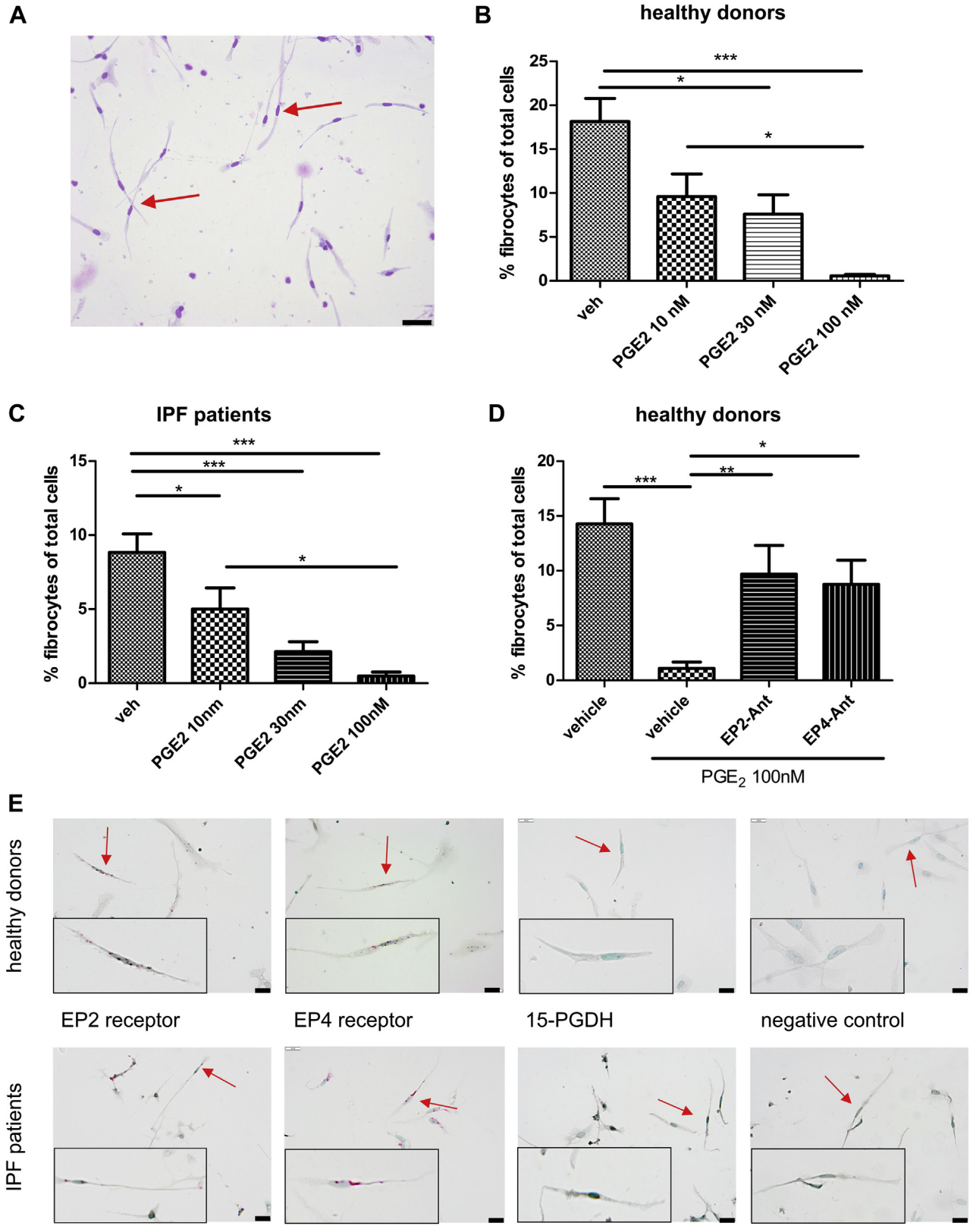

FIG 5. *In vitro* fibrocyte differentiation is abrogated by PGE_2 in healthy donors and patients with IPF. Fibrocytes express EP2 and EP4 receptors but not 15-PGDH mRNA. **A,** PBMCs from healthy donors were differentiated and after 5 days, cells were stained with DiffQuick. Scale bar shows 50 μm. Fibrocytes from (**B** and **D**) healthy donors or (**C**) patients with IPF were counted and the effects of PGE_2, in the absence and presence of the EP2 antagonist (PF04418948 1 μmol) and the EP4 antagonist (ONO AE3 208 1 μmol), were determined. **E,** ISH for the indicated targets *(red dots)* on fibrocytes from *(upper row)* healthy donors and *(lower row)* patients with IPF was performed. Photomicrographs are representative for 4 donors. *Scale bars* show 20 μm. Fibrocytes are indicated by *red arrows*; insets show these cells. One-way ANOVA for repeated measurements, followed by Tukey test, was applied for (Fig 5, *B-D*) (n = 9). $*P < .05$, $**P < .01$, $***P < .001$.

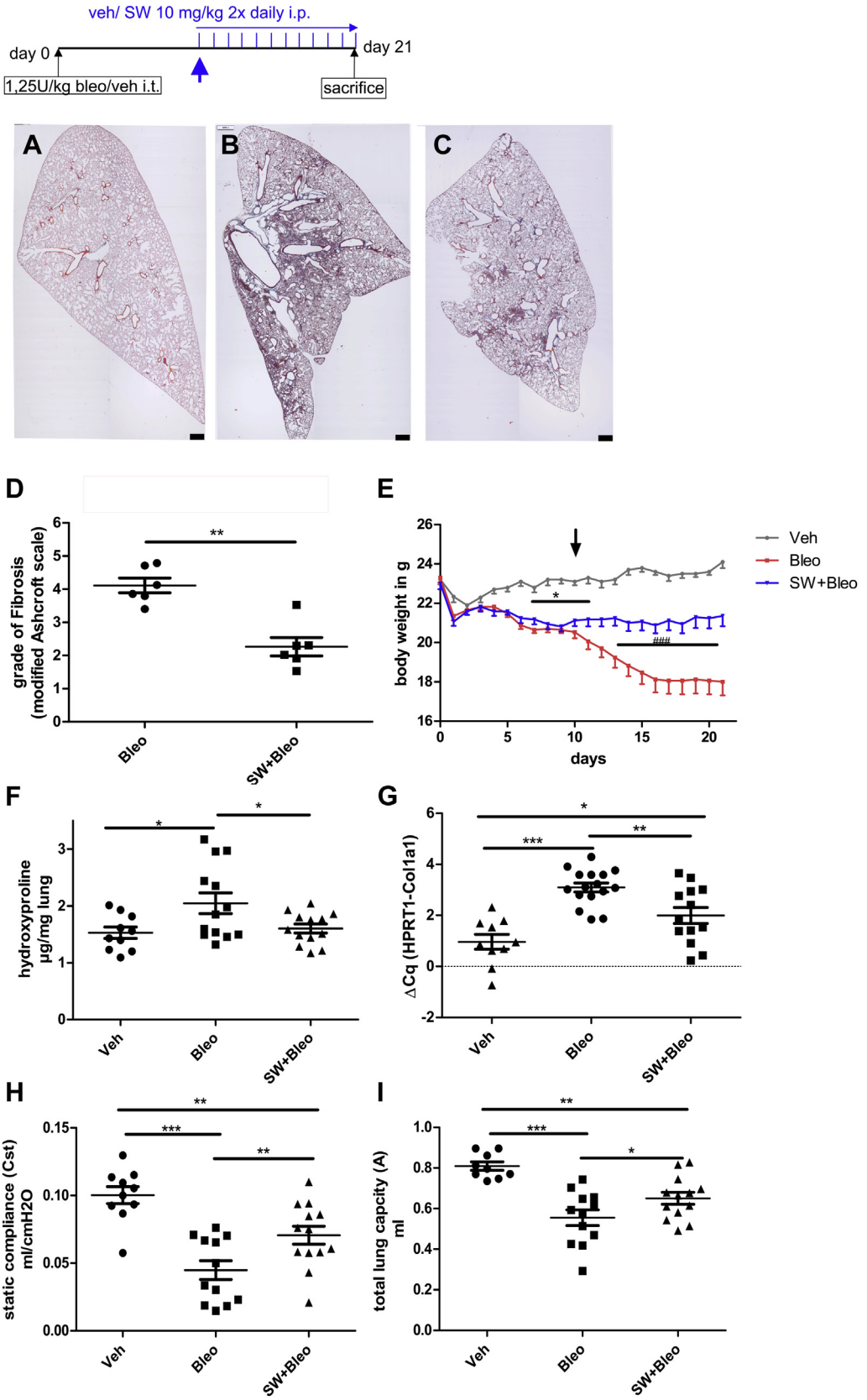

FIG 6. Inhibition of 15-PGDH ameliorates bleomycin-induced pulmonary fibrosis in a therapeutic model. **A-C,** Whole left lobes of mice treated with (Fig 6, *A*) vehicle (veh), (Fig 6, *B*) bleomycin (1.25 U/kg, Bleo), and (Fig 6, *C*) 15-PGDH inhibitor plus bleomycin (SW + Bleo; SW033291 10 mg/kg twice daily, from day 10 onward) were stained with Masson's trichrome. *Scale bars* indicate 1 mm. **D,** Grade of fibrosis was

(Fig 6, *A-D*), although not to the extent observed in the preventive model (cf Fig 2, *D*). Again, animals treated with bleomycin showed a significant decrease in weight as compared with controls. However, the start of treatment with the 15-PGDH inhibitor after 11 days halted the weight loss immediately, whereas in the absence of the inhibitor, body weight further declined in bleomycin-treated mice (Fig 6, *E*). In agreement with this observation, 15-PGDH inhibition reduced hydroxyproline content and collagen type 1 α1 (Col1a1) mRNA (Fig 6, *F* and *G*), confirming our histologic findings (Fig 6, *A-D*). Importantly, lung function testing revealed a beneficial effect of 15-PGDH inhibition on static compliance and total lung capacity (Fig 6, *H* and *I*). Similar effects could also be observed with a structurally unrelated 15-PGDH inhibitor (Fig E6).

Expression of 15-PGDH is controlled by miRNA 218-5p *in vitro* and *in vivo*

Because miRNA 218-5p has recently been demonstrated to be crucial in the regulation of 15-PGDH and this miRNA is decreased in patients with IPF,[42-44] we wanted to know whether it colocalizes with 15-PGDH mRNA in human lungs. In fact, we found that both were present in the same cells in healthy human lung tissue (Fig 7, *A-D*). To gain insights into the function of this miRNA in the lung, we tested whether transfection of A549 cells with a specific mimetic or inhibitor of miRNA 218-5p influences 15-PGDH levels. Interestingly, we found a profound down- and upregulation of 15-PGDH mRNA levels, respectively, after 24 hours (Fig 7, *E*) and regulation on protein level at 24 to 72 hours (Fig 7, *F* and *H*). Because A549 cells are a cancer cell line and partly differ in their behavior from alveolar epithelial cells, especially with regard to prostanoid synthesis,[46,62] we also transfected C57/Bl6 mice *in vivo*. Also in mouse lungs, the 218-5p mimetic caused a significant downregulation of 15-PGDH protein after 24 hours (Fig 7, *G* and *I*). Interestingly, TargetScan version 7.2 (http://www.targetscan.org),[63] a platform that predicts biological targets of miRNAs, revealed another conserved candidate miRNA, miRNA 26a-5p, that could regulate 15-PGDH expression and is decreased in IPF.[42-44] We also found that a mimic of this miRNA, which has already been proven to be therapeutically effective in the bleomycin model,[64] decreases 15-PGDH expression in A549 cells (Fig E5). Furthermore, in a noncancerous human kidney cell line (HK2) both miRNA mimics significantly decreased 15-PGDH expression (Fig E5).

15-PGDH inhibition increases eicosanoid levels in PCLSs from end-stage IPF lungs

As 15-PGDH is decreased in scarred tissue in IPF and intact tissue becomes more and more scarce as the disease progresses, we wanted to investigate whether 15-PGDH inhibition is still sufficient to increase eicosanoid levels. PCLSs from patients with IPF who underwent lung transplantation still showed a concentration-dependent increase in PGE_2 levels after 72 hours of treatment with the 15-PGDH inhibitor SW033291 (Fig 8, *A*). Besides PGE_2, there was also a slight increase in $PGF_{2\alpha}$ and 6-keto-$PGF_{1\alpha}$, a stable PGI_2 metabolite (Fig 8, *D*). Furthermore, at concentrations that caused a significant increase in PGE_2, the 15-PGDH inhibitor also decreased Col1a1 concentrations as measured in the supernatants (Fig 8, *E*) and this was inversely correlated with the relative increase in PGE_2 (Fig 8, *F*).

DISCUSSION

In the present study, we showed that 15-PGDH expression is altered in IPF, possibly via miRNA-dependent mechanisms, and that 15-PGDH inhibition is both a preventive and therapeutic strategy in a mouse model of bleomycin-induced pulmonary fibrosis. In patients with IPF, we could observe a vast discrepancy between 2 different readouts. Although no increase in 15-PGDH activity in total lung lysates from patients with IPF was detected as compared with healthy controls, immunohistochemistry revealed abundant expression of 15-PGDH predominantly in preserved alveolar walls but not in fibrotic lesions in IPF lungs. A recent study[65] comparing the transcriptome of macroscopically scarred tissue and intact tissue from IPF and healthy donor lungs found very similar results, that is, an increase in 15-PGDH in normal-appearing IPF tissue as compared with healthy controls and a subsequent decrease in scarred IPF tissue. These results highlight the influence of the spatial and temporal heterogeneity of IPF on commonly used readouts and urge caution in this process. Our results complement earlier findings describing impaired COX-2 expression in IPF fibroblasts and tissue[24-26,66] but pronounced staining for COX-2 especially in nonfibrotic areas and metaplastic epithelium of fibroblastic foci.[27,28] Therefore, it can be hypothesized that the combination of lower PGE_2 synthesis by IPF fibroblasts and the increased expression of 15-PGDH in tissue with preserved architecture, mainly in intact alveolar walls, contributes to the decreased levels of PGE_2 in IPF BAL fluid.[22] Consistently, increased concentrations of PGE-major urinary metabolites as found in patients with IPF[28] might be explained by the pronounced COX-2 expression (and probably also increased PG synthesis) in metaplastic epithelium and increased degradation of PGE_2 by 15-PGDH.

It has been described that 15-PGDH expression is under the control of miRNA 218-5p.[44] We could show that 15-PGDH is also regulated by mimics of this miRNA in A549 cells as well as in mouse lungs and that inhibition of miRNA 218-5p caused an increase in 15-PGDH protein and mRNA levels in A549 cells. We therefore assume that the decreased miRNA 218-5p expression that has been observed in patients with IPF[42,43] contributes to the subsequent partial upregulation of 15-PGDH. This finding goes well with the facts that TGF-β stimulation of

determined on 60 to 70 photomicrographs of the whole lung at a 200 × magnification and scored on the basis of a modified Ashcroft scale in a double-blind fashion. **E,** Body weight was measured daily and last observation was carried forward. **F,** Hydroxyproline levels, as a measure for lung collagen, were assayed from pulverized lung homogenates. **G,** Quantitative PCR for Col1a1 was performed from lung homogenates and normalized to HPRT1 as a housekeeping gene. **H,** Static compliance was measured on day 21. **I,** Total lung capacity was measured on day 21. For Fig 6, *D*, Mann-Whitney *U* test was performed (n = 6). One-way ANOVA, followed by Newman-Keuls test, was applied for Fig 6, *F* to *I* (n = 9-16). For Fig 6, *E*, 2-way ANOVA for repeated measurements, followed by Bonferroni *post hoc* test, was applied (n = 9-16). **P* < .05, ***P* < .01, ****P* < .001; in (Fig 6, *E*) ##*P* < .01 SW + Bleo vs Bleo.

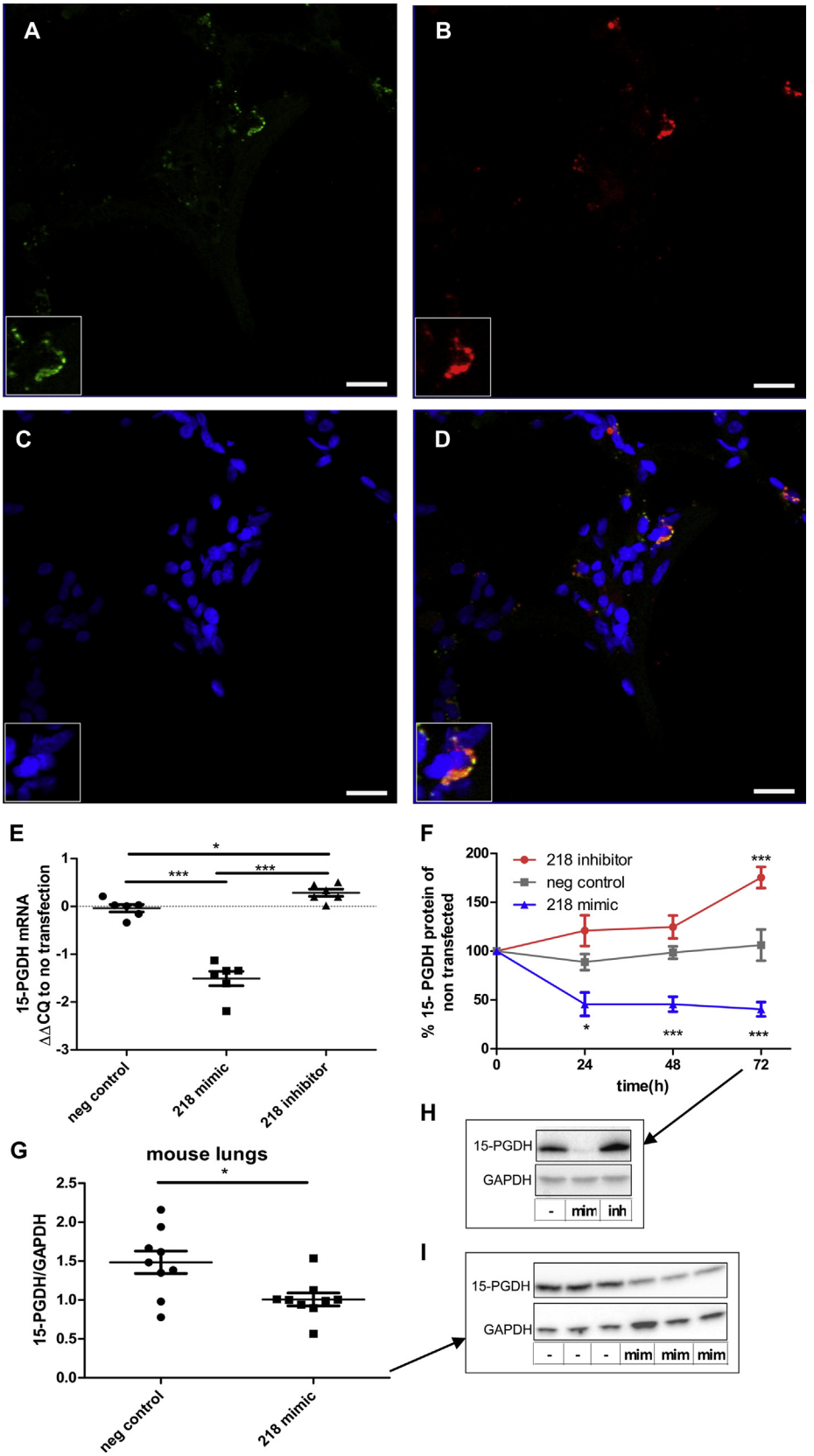

FIG 7. Pre-miRNA 218 and 15-PGDH mRNA are present in the same cells in healthy adult human lungs, and miRNA 218-5p regulates 15-PGDH *in vitro* and *in vivo*. **A-D,** ISH for (Fig 7, *A*) pre-miRNA 218a and (Fig 7, *B*) 15-PGDH mRNA was performed; sections were counterstained with (Fig 7, *C*) DAPI and (Fig 7, *D*) an overlay is shown. The image is representative for lungs of 5 healthy controls. *Scale bars* indicate 20 μm; insets show

A549 cells increased 15-PGDH[67] and decreased miRNA 218-5p levels.[68] Thus, it seems likely that at least in this cellular system 15-PGDH expression is regulated by miRNA 218-5p, although other factors, such as TGF-β, probably also play a role. Interestingly, both decreased miRNA 218-5p and increased 15-PGDH expression have been associated with a downregulation of epithelial cell markers and an upregulation of mesenchymal markers,[67,68] features that are hypothesized to play a role in IPF, although probably not in the sense of epithelial to mesenchymal transition.[69,70] Of note, we also found that a mimetic of miRNA 26a-5p, which is also downregulated in IPF and has been proven to be therapeutically efficient in the bleomycin model,[64] caused a downregulation of 15-PGDH in A549 cells.

In the bleomycin mouse model of pulmonary fibrosis, we confirmed the finding that bleomycin leads to increased PGE_2 concentrations,[9,12] but we also showed that inhibition of 15-PGDH still leads to a further significant increase. Analysis of common readouts revealed that the inhibitor treatment was sufficient to prevent fibrosis when started at day 0. This is in accordance with a host of data reporting protective effects of PGE_2 in the bleomycin model.[12,13,16,66] It has previously been described for PGE_2 that it decreases hydroxyproline content, ameliorates histologic changes, and reduces weight loss and mortality in bleomycin-treated mice.[12,13] In the present study we observed that inhibition of 15-PGDH also reduced fibrocyte counts in the mouse lung. Although EP receptors have been shown to be expressed in differentiated fibrocytes, and treprostinil, a prostacyclin analog, inhibits fibrocyte differentiation,[21] to our knowledge there are no data so far showing effects of PGE_2 on these cells. This is particularly interesting because fibrocytes are increased in the blood and lungs of patients with IPF as compared with healthy controls,[71] indicate poor prognosis,[72] and both pirfenidone and nintedanib decrease fibrocyte differentiation, migration, and fibrocyte counts *in vitro* and in mouse models.[20,57] The finding that PGE_2 decreased fibrocyte differentiation in PBMCs from healthy donors in an EP2 and EP4 receptor–dependent manner led us to investigate cells from patients with IPF, because alterations in EP2 receptor expression and signaling pathways have been described in IPF lung tissue, in patient-derived fibroblasts, and in the bleomycin mouse model, thereby reducing sensibility to the antifibrotic effects of PGE_2.[58,59,73,74] However, in our *in vitro* approach, we could see no such changes. PGE_2 reduced fibrocyte differentiation at similar concentrations as compared with healthy donors. Furthermore, the EP2 receptor was still expressed in patient-derived fibrocytes as confirmed by ISH. We therefore assume that fibrocytes are an additional target of the antifibrotic effects of PGE_2. In addition, we found that EP2 receptor protein and mRNA were still expressed in PCLSs (Fig E7).

In addition, we found profound effects of 15-PGDH inhibitor treatment on AT2 cells in the bleomycin model. Because apoptosis of AT2 cells has been implicated in fibrosis,[51] and their depletion via shortened telomeres might play a role in IPF,[75] we investigated whether increasing prostanoid concentration due to inhibition of 15-PGDH would alter this state. Although we found increased apoptosis and slightly increased proliferation of AT2 cells after bleomycin treatment in line with earlier studies,[54,56] the 15-PGDH inhibitor reduced AT2 cell apoptosis and increased proliferation. This complements earlier studies, describing antiapoptotic effects of PGE_2 on alveolar epithelial cell lines and involvement of PGE_2 in the "apoptosis paradox" in IPF,[11] meaning that it might counteract the pathognomonic features of increased alveolar epithelial cell and decreased fibroblast apoptosis.[8,11,76] This is also in line with the result that 15-PGDH inhibition led to a decrease in proliferating fibroblasts. In conclusion we hypothesize that the combination of protection from apoptosis and further induction of proliferation of AT2 cells together with the decreased fibroblast proliferation are at least partly responsible for the beneficial effects of our therapeutic approach in the bleomycin mouse model. Taken together, the data from the mouse model clearly indicate that inhibition of 15-PGDH is a valid strategy to achieve the beneficial effects of PGE_2, without the need to directly administer PGE_2 itself, which proved to be cumbersome.[77] This is further corroborated by the fact that COX inhibition reversed the effects of the 15-PGDH inhibitor (Fig E6).

Because of the promising *in vivo* data, we also set out to investigate the effects of 15-PGDH inhibition in PCLSs from patients with IPF. Therein we found a highly significant increase in PGE_2 even in end-stage explants, meaning under conditions in which intact tissue was strongly reduced and, therefore, smaller effects of 15-PGDH inhibition would be expected. Furthermore, we found that 15-PGDH inhibition led to a significant decrease in Col1a1 secretion, a finding that is well in line with our *in vivo* data and earlier reports regarding the inhibition of collagen secretion by PGE_2.[78] This decrease was inversely correlated with the relative increase in PGE_2 levels. Mass spectrometry also revealed an increase in $PGF_{2\alpha}$ levels, as would be expected because 15-PGDH is also a catabolic enzyme for this prostanoid, although with lower V_{max} and almost tripled K_m.[33] Also, 6-keto-$PGF_{1\alpha}$, the stable metabolite of PGI_2, showed a trend toward an increase, also in line with earlier observation,[79] and was the highest at the baseline conditions. The fact that we could not find specialized proresolving mediators in PCLS supernatants, although lipoxin A4 is a substrate of 15-PGDH,[35] is probably due to the transcellular pathway of lipoxin synthesis that usually involves immune cells[80] and due to the very low levels present without additional stimuli.[81]

A crucial finding in our study apparently contradicts an earlier report, which compared global 15-PGDH knockout mice with wild-type mice showing no effect on static compliance, tissue elastance, and septal thickening in the bleomycin model.[82] An important caveat of these findings concerns the genetic alteration

a double-positive cell. **E** and **F,** A549 cells were transfected with a mimic and an inhibitor of miRNA 218-5p, mRNA expression levels were measured (Fig 7, *E*) 24 hours later, and (Fig 7, *F*) a time course for 15-PGDH protein expression was performed. **H,** A representative Western blot at the 72-hour time point (− shows negative control, mimic shows miRNA 218a-5p mimic, and inhibitor shows miRNA 218a-5p inhibitor). **G,** Twenty-four hours after transfection of mouse lungs with a mimic for miRNA 218a-5p or negative control, lungs were harvested for Western blot analysis of 15-PGDH. In Fig 7, *E*, a representative Western blot is shown. For *E*, 1-way ANOVA, followed by Newman-Keuls test, was performed. For *F*, 2-way ANOVA, followed by Bonferroni *post hoc* test, was done. For *G*, Student *t* test was performed. $*P < .05$, $**P < .01$, $***P < .001$.

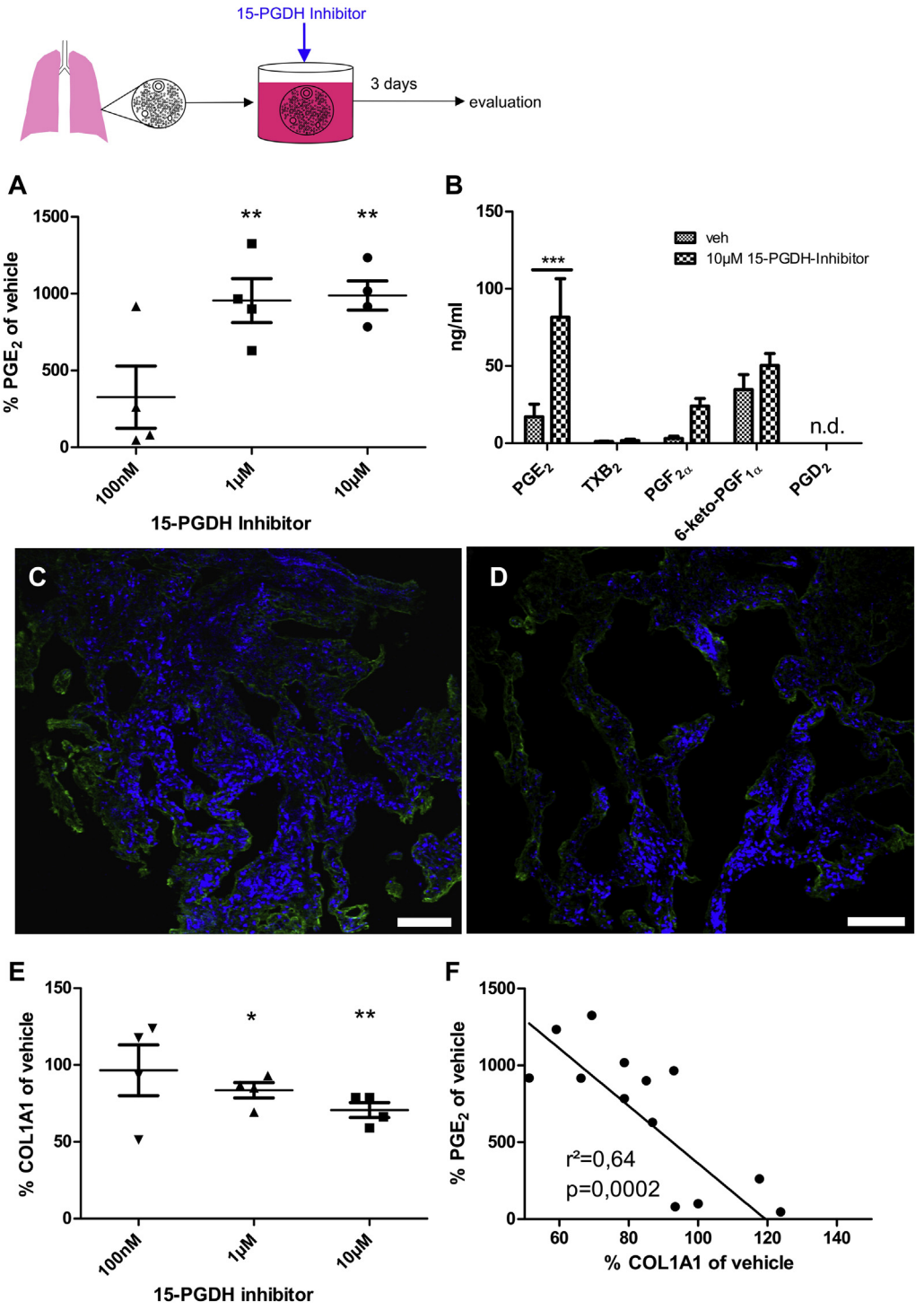

FIG 8. Inhibition of 15-PGDH increases PGE_2 levels and decreases collagen secretion in PCLSs from patients with IPF. PCLSs from patients with IPF were incubated with a 15-PGDH inhibitor (SW033291) at the indicated concentrations for 72 hours, and thereafter (**A**) PGE_2 (radioimmunoassay), (**B**) eicosanoid (mass spectrometry), and (**E**) Col1a1 (ELISA) levels were measured in the supernatants. **F,** Linear regression analysis was performed. Col1a1 was stained on PCLSs treated with (**C**) vehicle or (**D**) 15-PGDH inhibitor (SW033291, 10 μM); scale bar is 100 μm. For Fig 8, *A* and *E*, a 2-tailed 1-sample *t* test against 100% was performed. For *B*, 2-way ANOVA for repeated measurements, followed by Bonferroni *post hoc* test, was applied. *n.d.*, Not detected. $*P < .05$, $**P < .01$, $***P < .001$.

of PG biosynthesis, which has recently been stressed in a workshop report asking for caution with pharmacological studies in IPF mouse models.[61] Our data clearly demonstrate that pharmacologic inhibition of 15-PGDH is beneficial in a therapeutic model in mice (where the therapeutic agent is given only in the fibrotic phase, when inflammation abates), which is in agreement with results of a metabolically stable PGE_2 analog,[83] which also ameliorated lung function and reduced hydroxyproline content (a measure of collagen) in the bleomycin model.[61]

In conclusion, our data show that the inhibition of 15-PGDH results in a pronounced therapeutic effect in a mouse model of pulmonary fibrosis and abrogates collagen secretion in human PCLSs, and that PGE_2 reduces fibrocyte differentiation. We show alterations in 15-PGDH expression and in regulatory pathways, governing 15-PGDH levels in IPF. We therefore suggest 15-PGDH as a novel therapeutic target in IPF, a condition that still has limited therapeutic options and high mortality.

We thank Markus Absenger-Novak and Eleonore Fröhlich from the core facility for microscopy of the Medical University Graz for their expert assistance in image acquisition. We are particularly grateful to Martina Ofner, Sabine Kern, Sabine Halsegger, Daniela Kleinschek, Wolfgang Platzer, and Kathrin Rohrer for their expert technical assistance.

Key messages

- **15-Prostaglandin dehydrogenase expression is altered in idiopathic pulmonary fibrosis (IPF) lungs.**
- **Inhibition of this enzyme exerts beneficial effects via increasing levels of prostaglandin E_2, a potent antifibrotic mediator.**
- **Inhibitor treatment ameliorates established fibrosis in an animal model of IPF and decreases collagen production in IPF lungs.**
- **Prostaglandin E_2 inhibits fibrocyte differentiation.**

REFERENCES

1. Raghu G, Collard HR, Egan JJ, Martinez FJ, Behr J, Brown KK, et al. An official ATS/ERS/JRS/ALAT statement: idiopathic pulmonary fibrosis: evidence-based guidelines for diagnosis and management. Am J Respir Crit Care Med 2011; 183:788-824.
2. Bjoraker JA, Ryu JH, Edwin MK, Myers JL, Tazelaar HD, Schroeder DR, et al. Prognostic significance of histopathologic subsets in idiopathic pulmonary fibrosis. Am J Respir Crit Care Med 1998;157:199-203.
3. Raghu G, Chen SY, Yeh WS, Maroni B, Li Q, Lee YC, et al. Idiopathic pulmonary fibrosis in US Medicare beneficiaries aged 65 years and older: incidence, prevalence, and survival, 2001-11. Lancet Respir Med 2014;2:566-72.
4. Rafii R, Juarez MM, Albertson TE, Chan AL. A review of current and novel therapies for idiopathic pulmonary fibrosis. J Thorac Dis 2013;5:48-73.
5. Gomer RH. New approaches to modulating idiopathic pulmonary fibrosis. Curr Allergy Asthma Rep 2013;13:607-12.
6. King TE Jr, Bradford WZ, Castro-Bernardini S, Fagan EA, Glaspole I, Glassberg MK, et al. A phase 3 trial of pirfenidone in patients with idiopathic pulmonary fibrosis. N Engl J Med 2014;370:2083-92.
7. George G, Vaid U, Summer R. Therapeutic advances in idiopathic pulmonary fibrosis. Clin Pharmacol Ther 2016;99:30-2.
8. Bozyk PD, Moore BB. Prostaglandin E2 and the pathogenesis of pulmonary fibrosis. Am J Respir Cell Mol Biol 2011;45:445-52.
9. Oga T, Matsuoka T, Yao C, Nonomura K, Kitaoka S, Sakata D, et al. Prostaglandin F(2alpha) receptor signaling facilitates bleomycin-induced pulmonary fibrosis independently of transforming growth factor-beta. Nat Med 2009;15:1426-30.
10. Lama V, Moore BB, Christensen P, Toews GB, Peters-Golden M. Prostaglandin E2 synthesis and suppression of fibroblast proliferation by alveolar epithelial cells is cyclooxygenase-2-dependent. Am J Respir Cell Mol Biol 2002;27:752-8.
11. Maher TM, Evans IC, Bottoms SE, Mercer PF, Thorley AJ, Nicholson AG, et al. Diminished prostaglandin E2 contributes to the apoptosis paradox in idiopathic pulmonary fibrosis. Am J Respir Crit Care Med 2010;182:73-82.
12. Dackor RT, Cheng J, Voltz JW, Card JW, Ferguson CD, Garrett RC, et al. Prostaglandin E(2) protects murine lungs from bleomycin-induced pulmonary fibrosis and lung dysfunction. Am J Physiol Lung Cell Mol Physiol 2011;301: L645-55.
13. Ivanova V, Garbuzenko OB, Reuhl KR, Reimer DC, Pozharov VP, Minko T. Inhalation treatment of pulmonary fibrosis by liposomal prostaglandin E2. Eur J Pharm Biopharm 2013;84:335-44.
14. Epa AP, Thatcher TH, Pollock SJ, Wahl LA, Lyda E, Kottmann RM, et al. Normal human lung epithelial cells inhibit transforming growth factor-beta induced myofibroblast differentiation via prostaglandin E2. PLoS One 2015;10: e0135266.
15. Ando M, Murakami Y, Kojima F, Endo H, Kitasato H, Hashimoto A, et al. Retrovirally introduced prostaglandin D2 synthase suppresses lung injury induced by bleomycin. Am J Respir Cell Mol Biol 2003;28:582-91.
16. Yoon YS, Lee YJ, Choi YH, Park YM, Kang JL. Macrophages programmed by apoptotic cells inhibit epithelial-mesenchymal transition in lung alveolar epithelial cells via PGE2, PGD2, and HGF. Sci Rep 2016;6:20992.
17. Roach KM, Feghali-Bostwick CA, Amrani Y, Bradding P. Lipoxin A4 attenuates constitutive and TGF-beta1-dependent profibrotic activity in human lung myofibroblasts. J Immunol 2015;195:2852-60.
18. Martins V, Valenca SS, Farias-Filho FA, Molinaro R, Simoes RL, Ferreira TP, et al. ATLa, an aspirin-triggered lipoxin A4 synthetic analog, prevents the inflammatory and fibrotic effects of bleomycin-induced pulmonary fibrosis. J Immunol 2009;182: 5374-81.
19. Guilherme RF, Xisto DG, Kunkel SL, Freire-de-Lima CG, Rocco PR, Neves JS, et al. Pulmonary antifibrotic mechanisms aspirin-triggered lipoxin A(4) synthetic analog. Am J Respir Cell Mol Biol 2013;49:1029-37.
20. Sato S, Shinohara S, Hayashi S, Morizumi S, Abe S, Okazaki H, et al. Anti-fibrotic efficacy of nintedanib in pulmonary fibrosis via the inhibition of fibrocyte activity. Respir Res 2017;18:172.
21. Nikam VS, Wecker G, Schermuly R, Rapp U, Szelepusa K, Seeger W, et al. Treprostinil inhibits the adhesion and differentiation of fibrocytes via the cyclic adenosine monophosphate-dependent and Ras-proximate protein-dependent inactivation of extracellular regulated kinase. Am J Respir Cell Mol Biol 2011; 45:692-703.
22. Borok Z, Gillissen A, Buhl R, Hoyt RF, Hubbard RC, Ozaki T, et al. Augmentation of functional prostaglandin E levels on the respiratory epithelial surface by aerosol administration of prostaglandin E. Am Rev Respir Dis 1991; 144:1080-4.
23. Huang SK, Peters-Golden M. Eicosanoid lipid mediators in fibrotic lung diseases: ready for prime time? Chest 2008;133:1442-50.
24. Wilborn J, Crofford LJ, Burdick MD, Kunkel SL, Strieter RM, Peters-Golden M. Cultured lung fibroblasts isolated from patients with idiopathic pulmonary fibrosis have a diminished capacity to synthesize prostaglandin E2 and to express cyclooxygenase-2. J Clin Invest 1995;95:1861-8.
25. Xaubet A, Roca-Ferrer J, Pujols L, Ramirez J, Mullol J, Marin-Arguedas A, et al. Cyclooxygenase-2 is up-regulated in lung parenchyma of chronic obstructive pulmonary disease and down-regulated in idiopathic pulmonary fibrosis. Sarcoidosis Vasc Diffuse Lung Dis 2004;21:35-42.
26. Evans IC, Barnes JL, Garner IM, Pearce DR, Maher TM, Shiwen X, et al. Epigenetic regulation of cyclooxygenase-2 by methylation of c8orf4 in pulmonary fibrosis. Clin Sci 2016;130:575-86.
27. Lappi-Blanco E, Kaarteenaho-Wiik R, Maasilta PK, Anttila S, Paakko P, Wolff HJ. COX-2 is widely expressed in metaplastic epithelium in pulmonary fibrous disorders. Am J Clin Pathol 2006;126:717-24.
28. Horikiri T, Hara H, Saito N, Araya J, Takasaka N, Utsumi H, et al. Increased levels of prostaglandin E-major urinary metabolite (PGE-MUM) in chronic fibrosing interstitial pneumonia. Respir Med 2017;122:43-50.
29. Petkova DK, Clelland CA, Ronan JE, Lewis S, Knox AJ. Reduced expression of cyclooxygenase (COX) in idiopathic pulmonary fibrosis and sarcoidosis. Histopathology 2003;43:381-6.
30. Hodges RJ, Jenkins RG, Wheeler-Jones CP, Copeman DM, Bottoms SE, Bellingan GJ, et al. Severity of lung injury in cyclooxygenase-2-deficient mice is dependent on reduced prostaglandin E(2) production. Am J Pathol 2004;165: 1663-76.
31. Card JW, Voltz JW, Carey MA, Bradbury JA, Degraff LM, Lih FB, et al. Cyclooxygenase-2 deficiency exacerbates bleomycin-induced lung dysfunction but not fibrosis. Am J Respir Cell Mol Biol 2007;37:300-8.

32. Cheng J, Dackor RT, Bradbury JA, Li H, DeGraff LM, Hong LK, et al. Contribution of alveolar type II cell-derived cyclooxygenase-2 to basal airway function, lung inflammation, and lung fibrosis. FASEB J 2016;30:160-73.
33. Nakano J, Anggard E, Samuelsson B. 15-Hydroxy-prostanoate dehydrogenase. Prostaglandins as substrates and inhibitors. Eur J Biochem 1969;11:386-9.
34. Tai HH, Ensor CM, Tong M, Zhou H, Yan F. Prostaglandin catabolizing enzymes. Prostaglandins Other Lipid Mediat 2002;68-69:483-93.
35. Clish CB, Levy BD, Chiang N, Tai HH, Serhan CN. Oxidoreductases in lipoxin A4 metabolic inactivation: a novel role for 15-onoprostaglandin 13-reductase/leukotriene B4 12-hydroxydehydrogenase in inflammation. J Biol Chem 2000;275:25372-80.
36. Bergmann C, Wobser M, Morbach H, Falkenbach A, Wittenhagen D, Lassay L, et al. Primary hypertrophic osteoarthropathy with digital clubbing and palmoplantar hyperhidrosis caused by 15-PGHD/HPGD loss-of-function mutations. Exp Dermatol 2011;20:531-3.
37. Seifert W, Beninde J, Hoffmann K, Lindner TH, Bassir C, Aksu F, et al. HPGD mutations cause cranioosteoarthropathy but not autosomal dominant digital clubbing. Eur J Hum Genet 2009;17:1570-6.
38. Coggins KG, Latour A, Nguyen MS, Audoly L, Coffman TM, Koller BH. Metabolism of PGE2 by prostaglandin dehydrogenase is essential for remodeling the ductus arteriosus. Nat Med 2002;8:91-2.
39. Jiang W, Upadhyaya P, Zhang W, Yu G, Jungfleisch MB, Fradin FY, et al. Magnetism. Blowing magnetic skyrmion bubbles. Science 2015;349:283-6.
40. Fernandez IE, Eickelberg O. The impact of TGF-beta on lung fibrosis: from targeting to biomarkers. Proc Am Thorac Soc 2012;9:111-6.
41. Yan M, Rerko RM, Platzer P, Dawson D, Willis J, Tong M, et al. 15-Hydroxyprostaglandin dehydrogenase, a COX-2 oncogene antagonist, is a TGF-beta-induced suppressor of human gastrointestinal cancers. Proc Natl Acad Sci U S A 2004;101:17468-73.
42. Pandit KV, Corcoran D, Yousef H, Yarlagadda M, Tzouvelekis A, Gibson KF, et al. Inhibition and role of let-7d in idiopathic pulmonary fibrosis. Am J Respir Crit Care Med 2010;182:220-9.
43. Berschneider B, Ellwanger DC, Baarsma HA, Thiel C, Shimbori C, White ES, et al. miR-92a regulates TGF-beta1-induced WISP1 expression in pulmonary fibrosis. Int J Biochem Cell Biol 2014;53:432-41.
44. Cong R, Tao K, Fu P, Lou L, Zhu Y, Chen S, et al. MicroRNA218 promotes prostaglandin E2 to inhibit osteogenic differentiation in synovial mesenchymal stem cells by targeting 15hydroxyprostaglandin dehydrogenase [NAD(+)]. Mol Med Rep 2017;16:9347-54.
45. Rayamajhi M, Redente EF, Condon TV, Gonzalez-Juarrero M, Riches DW, Lenz LL. Non-surgical intratracheal instillation of mice with analysis of lungs and lung draining lymph nodes by flow cytometry. J Vis Exp 2011;51.
46. Barnthaler T, Maric J, Platzer W, Konya V, Theiler A, Hasenohrl C, et al. The role of PGE2 in alveolar epithelial and lung microvascular endothelial crosstalk. Sci Rep 2017;7:7923.
47. Schlosser K, Taha M, Stewart DJ. Systematic assessment of strategies for lung-targeted delivery of microRNA mimics. Theranostics 2018;8:1213-26.
48. Taira A, Nishimura M, Amako H, Otsubo M, Kodama H. Evaluation of mitral commissurotomy in 5- to 15-year follow-up [in Japanese] . Nihon Kyobu Geka Gakkai Zasshi 1976;24:1127-33.
49. Martin C, Uhlig S, Ullrich V. Videomicroscopy of methacholine-induced contraction of individual airways in precision-cut lung slices. Eur Respir J 1996;9:2479-87.
50. Pilling D, Gomer RH. Differentiation of circulating monocytes into fibroblast-like cells. Methods Mol Biol 2012;904:191-206.
51. Barbas-Filho JV, Ferreira MA, Sesso A, Kairalla RA, Carvalho CR, Capelozzi VL. Evidence of type II pneumocyte apoptosis in the pathogenesis of idiopathic pulmonary fibrosis (IFP)/usual interstitial pneumonia (UIP). J Clin Pathol 2001;54:132-8.
52. Aguilar S, Scotton CJ, McNulty K, Nye E, Stamp G, Laurent G, et al. Bone marrow stem cells expressing keratinocyte growth factor via an inducible lentivirus protects against bleomycin-induced pulmonary fibrosis. PLoS One 2009;4:e8013.
53. Fan Y, Wang Y, Wang K. Prostaglandin E2 stimulates normal bronchial epithelial cell growth through induction of c-Jun and PDK1, a kinase implicated in oncogenesis. Respir Res 2015;16:149.
54. Safaeian L, Jafarian-Dehkordi A, Rabbani M, Sadeghi HM, Afshar-Moghaddam N, Sarahroodi S. Comparison of bleomycin-induced pulmonary apoptosis between NMRI mice and C57BL/6 mice. Res Pharm Sci 2013;8:43-50.
55. Jordana M, Schulman J, McSharry C, Irving LB, Newhouse MT, Jordana G, et al. Heterogeneous proliferative characteristics of human adult lung fibroblast lines and clonally derived fibroblasts from control and fibrotic tissue. Am Rev Respir Dis 1988;137:579-84.
56. Mikamo M, Kitagawa K, Sakai S, Uchida C, Ohhata T, Nishimoto K, et al. Inhibiting Skp2 E3 ligase suppresses bleomycin-induced pulmonary fibrosis. Int J Mol Sci 2018;19.
57. Inomata M, Kamio K, Azuma A, Matsuda K, Kokuho N, Miura Y, et al. Pirfenidone inhibits fibrocyte accumulation in the lungs in bleomycin-induced murine pulmonary fibrosis. Respir Res 2014;15:16.
58. Moore BB, Ballinger MN, White ES, Green ME, Herrygers AB, Wilke CA, et al. Bleomycin-induced E prostanoid receptor changes alter fibroblast responses to prostaglandin E2. J Immunol 2005;174:5644-9.
59. Okunishi K, Sisson TH, Huang SK, Hogaboam CM, Simon RH, Peters-Golden M. Plasmin overcomes resistance to prostaglandin E2 in fibrotic lung fibroblasts by reorganizing protein kinase A signaling. J Biol Chem 2011;286:32231-43.
60. Moeller A, Ask K, Warburton D, Gauldie J, Kolb M. The bleomycin animal model: a useful tool to investigate treatment options for idiopathic pulmonary fibrosis? Int J Biochem Cell Biol 2008;40:362-82.
61. Jenkins RG, Moore BB, Chambers RC, Eickelberg O, Konigshoff M, Kolb M, et al. An official American Thoracic Society Workshop report: use of animal models for the preclinical assessment of potential therapies for pulmonary fibrosis. Am J Respir Cell Mol Biol 2017;56:667-79.
62. Mitchell JA, Belvisi MG, Akarasereenont P, Robbins RA, Kwon OJ, Croxtall J, et al. Induction of cyclo-oxygenase-2 by cytokines in human pulmonary epithelial cells: regulation by dexamethasone. Br J Pharmacol 1994;113:1008-14.
63. Agarwal V, Bell GW, Nam JW, Bartel DP. Predicting effective microRNA target sites in mammalian mRNAs. Elife 2015;4.
64. Liang H, Xu C, Pan Z, Zhang Y, Xu Z, Chen Y, et al. The antifibrotic effects and mechanisms of microRNA-26a action in idiopathic pulmonary fibrosis. Mol Ther 2014;22:1122-33.
65. Luzina IG, Salcedo MV, Rojas-Pena ML, Wyman AE, Galvin JR, Sachdeva A, et al. Transcriptomic evidence of immune activation in macroscopically normal-appearing and scarred lung tissues in idiopathic pulmonary fibrosis. Cell Immunol 2018;325:1-13.
66. Bauman KA, Wettlaufer SH, Okunishi K, Vannella KM, Stoolman JS, Huang SK, et al. The antifibrotic effects of plasminogen activation occur via prostaglandin E2 synthesis in humans and mice. J Clin Invest 2010;120:1950-60.
67. Tai HH, Tong M, Ding Y. 15-Hydroxyprostaglandin dehydrogenase (15-PGDH) and lung cancer. Prostaglandins Other Lipid Mediat 2007;83:203-8.
68. Shi ZM, Wang L, Shen H, Jiang CF, Ge X, Li DM, et al. Downregulation of miR-218 contributes to epithelial-mesenchymal transition and tumor metastasis in lung cancer by targeting Slug/ZEB2 signaling. Oncogene 2017;36:2577-88.
69. Nieto MA, Huang RY, Jackson RA, Thiery JP. Emt: 2016. Cell 2016;166:21-45.
70. Rock JR, Barkauskas CE, Cronce MJ, Xue Y, Harris JR, Liang J, et al. Multiple stromal populations contribute to pulmonary fibrosis without evidence for epithelial to mesenchymal transition. Proc Natl Acad Sci U S A 2011;108:E1475-83.
71. Heukels P, van Hulst JAC, van Nimwegen M, Boorsma CE, Melgert BN, van den Toorn LM, et al. Fibrocytes are increased in lung and peripheral blood of patients with idiopathic pulmonary fibrosis. Respir Res 2018;19:90.
72. Moeller A, Gilpin SE, Ask K, Cox G, Cook D, Gauldie J, et al. Circulating fibrocytes are an indicator of poor prognosis in idiopathic pulmonary fibrosis. Am J Respir Crit Care Med 2009;179:588-94.
73. Mukherjee S, Sheng W, Michkov A, Sriarm K, Sun R, Dvorkin-Gheva A, et al. Prostaglandin E2 inhibits pro-fibrotic function of human pulmonary fibroblasts by disrupting Ca2+-signaling. Am J Physiol Lung Cell Mol Physiol 2019;316:L810-21.
74. Huang SK, Fisher AS, Scruggs AM, White ES, Hogaboam CM, Richardson BC, et al. Hypermethylation of PTGER2 confers prostaglandin E2 resistance in fibrotic fibroblasts from humans and mice. Am J Pathol 2010;177:2245-55.
75. Snetselaar R, van Batenburg AA, van Oosterhout MFM, Kazemier KM, Roothaan SM, Peeters T, et al. Short telomere length in IPF lung associates with fibrotic lesions and predicts survival. PLoS One 2017;12:e0189467.
76. Huang SK, White ES, Wettlaufer SH, Grifka H, Hogaboam CM, Thannickal VJ, et al. Prostaglandin E(2) induces fibroblast apoptosis by modulating multiple survival pathways. FASEB J 2009;23:4317-26.
77. Huang SK. "Yap"-ing about the antifibrotic benefits of prostacyclin. Am J Respir Cell Mol Biol 2019;60:499-500.
78. Kolodsick JE, Peters-Golden M, Larios J, Toews GB, Thannickal VJ, Moore BB. Prostaglandin E2 inhibits fibroblast to myofibroblast transition via E. prostanoid receptor 2 signaling and cyclic adenosine monophosphate elevation. Am J Respir Cell Mol Biol 2003;29:537-44.
79. Jarabak J, Fried J. Comparison of substrate specificities of the human placental NAD- and NADP-linked 15-hydroxyprostaglandin dehydrogenases. Prostaglandins 1979;18:241-6.
80. Bannenberg G, Serhan CN. Specialized pro-resolving lipid mediators in the inflammatory response: an update. Biochim Biophys Acta 2010;1801:1260-73.
81. Bhavsar PK, Levy BD, Hew MJ, Pfeffer MA, Kazani S, Israel E, et al. Corticosteroid suppression of lipoxin A4 and leukotriene B4 from alveolar macrophages in severe asthma. Respir Res 2010;11:71.

82. Lovgren AK, Jania LA, Hartney JM, Parsons KK, Audoly LP, Fitzgerald GA, et al. COX-2-derived prostacyclin protects against bleomycin-induced pulmonary fibrosis. Am J Physiol Lung Cell Mol Physiol 2006; 291:L144-56.

83. Failla M, Genovese T, Mazzon E, Fruciano M, Fagone E, Gili E, et al. 16,16-Dimethyl prostaglandin E2 efficacy on prevention and protection from bleomycin-induced lung injury and fibrosis. Am J Respir Cell Mol Biol 2009;41: 50-8.

METHODS

Reagents

Chemicals were obtained from Sigma (Vienna, Austria) unless specified otherwise. PGE_2, CAY10638, and the EP4 antagonist ONO AE3-208 were from Cayman Chemical (Ann Arbor, Mich). Vectashield/4′,6-diamidino-2-phenylindole (DAPI) mounting medium as well as secondary antibodies and horseradish peroxidase (HRP)/alkaline phosphatase–conjugated streptavidin were obtained from Vector Laboratories (Burlingam, Calif). The EP2 antagonist PF04418948 was obtained from Tocris (Bristol, UK). MirVana miRNA mimics and inhibitors as well as transfection reagents were purchased from Thermo Fisher Scientific (Waltham, Mass). Primary antibodies were purchased from Merck Millipore (Burlington, Mass), Cell Signaling (Cambridge, UK), Santa Cruz (Santa Cruz, Calif), Abcam (Cambridge, UK), Jackson ImmunoResearch (Baltimore Pike, Pa), and Sigma. SW033291 was purchased from THP Medical Products (Vienna, Austria). SW033291 is a small molecule inhibitor of 15-PGDH with an apparent inhibition constant (Ki^{app}) of 0.1 nmol, which has been shown not to affect 2 closely related short-chain dehydrogenases (HSD17B10 and BDH2).[E1] A list of the antibodies used and their dilutions is presented in Table E1 in this article's Online Repository at www.jacionline.org.

Animals

Ten- to 12-week-old C57/Bl6 J mice were used for all animal experiments. All animal care complied with national and international guidelines. Mice were housed in individually ventilated cages (4-5 per cage) under controlled conditions of temperature (set point 21°C), air humidity (set point 50%), and a 12-hour light/dark cycle (lights on at 6:00 AM) and habituated to the environment for at least 1 week. Standard chow and water were provided *ad libitum*. Mice were randomly assigned before treatment. The experimental procedure used in this study was approved by the Austrian Federal Ministry of Science, Research and Economy (BMWFW-66.010/0142-WF/V/3b/2016) and performed in accordance with the European Communities Council Directive of November 24, 1986 (86/609/EEC).

Bleomycin model

In brief, mice were anesthetized with a mixture of ketamine (75 mg/kg) and xylazine (7.5 mg/kg) via intraperitoneal injection, and bleomycin or vehicle (saline solution) was instilled intratracheally with a Hamilton syringe at a dose of 1.25 U/kg. Body weight was measured daily. SW033291, a 15-PGDH inhibitor, was dissolved in Kolliphor/EtOH (1:2), diluted to the desired concentration in 5% glucose solution, and given intraperitoneally.[E1] In the preventive model, mice received SW033291 at a dose of 10 mg/kg or solvent twice daily starting from day 0. For the therapeutic model, mice were injected with inhibitor/vehicle starting on day 11 post bleomycin. Mice were either sacrificed for histology and collection of BAL fluid or subjected to lung function measurements in the therapeutic model on day 21 post bleomycin. After euthanizing mice with an overdose of pentobarbital (150 mg/kg intraperitoneally), the lung was perfused with PBS. For histologic assessment, whole lungs were excised, inflated with 4% paraformaldehyde, and paraffin-embedded, whereas for all other measurements a BAL was performed, and whole lungs were snap-frozen and subsequently pulverized in liquid nitrogen. For BAL, an 18G cannula was inserted into the trachea, and 1 mL of PBS containing 0.1 mmol EDTA was instilled into the lung and collected.[E2] Another 15-PGDH inhibitor, CAY10638, was applied in the therapeutic model. Because this compound is not easily soluble in water, 10 mg was dissolved in 400 μL dimethyl sulfoxide and 800 μL Kolliphor/EtOH (1:2) was added. Immediately before injecting, this was mixed with 6800 μL of 5% glucose solution and the respective dose was given intraperitoneally.

Lung function

Mice receiving the therapeutic treatment strategy were subjected to lung function measurements by the forced oscillation technique on the FlexiVent system (Scireq, Montreal, Calif) as previously described.[E3,E4] In brief, mice were anesthetized with ketamine (150 mg/kg) or xylazine (15 mg/kg) and after absence of pain responses, mice were connected to the ventilation unit and paralyzed with rocuronium bromide (5 mg/kg).[E5] Afterwards, snapshot perturbations, forced oscillation perturbation, and ramp-volume–regulated pressure-volume curves were calculated at least thrice per animal and values were averaged.[E4] Only measurements with a coefficient of variation higher than 0.95 were accepted.

Hydroxyproline assay

In brief, 10 to 15 mg of pulverized lung tissue was dissolved in 100 to 150 μL distilled water, and an equal volume of 12 N HCl was added. After incubation for 3 hours at 120°C, samples were centrifuged (10,000*g*, 3 minutes) and 5 μL of the supernatants was transferred to a 96-well plate. A hydroxyproline assay kit (BioVision, Milpitas, Calif) was used according to the manufacturer's instructions.

Fibrosis grading

Lung sections of 5 μm were deparaffinized and stained with Masson-Goldner-Trichrome staining kit (Carl Roth, Karlsruhe, Germany) with some modifications. Instead of light green SF yellowish, aniline blue solution (2.5 g/100 mL, 2% acetic acid, glacial) was used. Sixty to seventy photomicrographs at 200 × magnification covering all lobes were taken and evaluated in a double-blind fashion by a modified Ashcroft scale.[E6]

Real-time PCR

Pulverized lung tissue or A549 cells were dissolved in 1 mL of RNAzol RT or 500 μL of TRIZOL, respectively, and RNA isolated according to the manufacturer's instructions; 1 μg of total RNA was reverse-transcribed using the iScript cDNA Synthesis Kit (Bio-Rad, Vienna, Austria); real-time PCR was performed using SsoAdvanced Universal SYBR Green Supermix with PrimePCR SYBR Green Assay primers for human *HPGD* and glyceraldehyde 3-phosphate dehydrogenase (*GAPDH*) and mouse *Hpgd*, *Gapdh*, *Col1a1*, and *Hprt1* (all Bio-Rad), according to the manufacturer's instructions (CDX Connect Real-time PCR detection system with CFX Manager software 3.1; Bio-Rad, Hercules, Calif). Samples were measured in duplicates, and *GAPDH* (A549 cells) and *Gapdh* and *Hprt1* (mouse lung) were used as reference genes. Quantification of mRNA expression relative to vehicle was calculated with the $2^{-\Delta\Delta CT}$ method (A549 cells) and as housekeeping gene minus gene of interest (mouse lung).

Immunohistochemistry/immunofluorescence

In brief, sections were subjected to deparaffinization and heat-mediated antigen retrieval (citrate, pH 6, 2 × 5 minutes in the microwave), blocked with 4% BSA and 10% secondary antibody host serum in PBS/0.3% Triton X, and stained overnight with primary antibody/antibodies. For immunofluorescence, sections were then incubated with fluorochrome-labeled secondary antibodies raised in goat, whereas for immunohistochemistry, matching VECTASTAIN kits (Vector Laboratories) were used according to the manufacturer's instructions. For immunohistochemical double labelings, HRP with 3,3'-diaminobenzidine (DAB) substrate and alkaline phosphatase with Vector Red was applied (Vector Laboratories).[E7] Methyl green was used as a counterstain, and sections were dehydrated and mounted with Histokit II (Carl Roth). Immunofluorescence sections were mounted in DAPI mounting medium. All stainings of human samples were performed according to an approved protocol by the Ethics Committee of the Medical University of Graz (29-014 ex 16/17). When combining with ISH, ISH was performed first, and immunofluorescence was started from the blocking step as described earlier. Sections were incubated with TrueView autofluorescence quenching kit, followed by mounting with DAPI HardSet (Vector Laboratories).

miRNA transfection

A549 cells were grown to confluence in Dulbecco modified Eagle medium, containing 10% FCS and 2 mmol L-glutamine. For 24-well plates, 6-fold

concentrated miRNA (as calculated from final concentration) was added to 100 μL Opti-minimum essential medium (MEM) followed by 1 μL of Lipofectamine RNAiMAX reagent. After mixing, followed by incubation for 20 minutes at room temperature, 30,000 passaged A549 cells were added in 500 μL of medium and the plate was rocked back and forth. The final concentration of miRNA mimic, inhibitor, and negative control was 30 nmol. Cells were harvested at indicated time points in TRIZOL for quantification of mRNA and in radioimmunoprecipitation assay (RIPA) buffer for Western blot analysis.

In brief, for a single dose, 2.5 μL of miRNA mimic stock (50 μmol)/negative control stock (50 μmol) was mixed with 2.5 μL of complexation buffer, and 5 μL of Invivofectamine was added. The solution was vortexed and incubated at 50°C for 30 minutes. Afterwards, this was diluted with 50 μL of sterile PBS, resulting in a final concentration of 2.08 μmol. The mice received 50 μL by intratracheal instillation once as described earlier, resulting in a delivery of 58 ng mimic/mg body weight.[E8] After 24 hours, lungs were perfused, snap-frozen, and subsequently pulverized in liquid nitrogen. Ten milligram of powder was dissolved in RIPA buffer and subjected to Western blotting.

Western blot

Briefly, cells or tissues were lysed in RIPA buffer, containing protease inhibitor cocktail (Roche, Basel, Switzerland) and 1 mmol phenylmethylsulfonyl fluoride, and protein content was analyzed using the Pierce BCA kit (Thermo Fisher Scientific) and 15 μg protein per sample was separated by SDS-PAGE on a 4% to 20% TRIS-glycine gradient gel (Thermo Fisher Scientific). Protein was then blotted using the iBlot dry transfer system (Thermo Fisher Scientific) on a polyvinylidene fluoride membrane, and thereafter the membrane was blocked (5% nonfat dry milk) for 1 hour and incubated with primary antibodies overnight. Secondary HRP-conjugated antibodies followed by HRP-detection substrate (Bio-Rad) were used to visualize chemoluminescence by ChemiDoc Touch Imaging system (Bio-Rad). After stripping with stripping buffer (Restore PLUS, Thermo Fisher Scientific), membranes were reprobed with a GAPDH antibody and processed as described earlier. Densitometric analysis of protein bands was performed using Imagelab Software (Bio-Rad).

15-PGDH activity assay

Pulverized lung tissue was transferred to 0.1 mol of potassium phosphate buffer (pH 7.5) and homogenized by a sonicator. After a first centrifugation step (20 minutes, 10,000*g*), the resulting supernatant was subjected to ultracentrifugation (60 minutes, 105,000*g*) and the final supernatant was used for the assay. Briefly, 100 μL was added to the reaction mix (50 mmol TRIS/HCl, 5 mmol NH_4Cl, 100 μmol ketoglutarate monosodium salt, 1 mmol nicotinamide adenine dinucleotide (NAD)+, 0.1 mmol dithiothreitol, and 5 U glutamate dehydrogenase) and the reaction was started by addition of heptatritiated PGE_2 (PerkinElmer, Waltham, Mass). After 30 minutes, 300 μL of 10% activated charcoal and 1% dextran (T70) were added, vials were centrifuged, and the resultant supernatant was poured into scintillation tubes. Counts per minute were determined on a beta counter (Beckman Coulter, Brea, Calif). For quantification, a standard curve of purified enzyme was prepared.

Precision cut lung slices

The applied protocol and the usage of the tissue were approved by the institutional ethics committee (976/2010) of the Medical University of Vienna, and patients' informed consent was obtained before lung transplantation. Fresh lung specimens were obtained from 4 patients with IPF undergoing lung transplantation. Cylindrical cores (8 mm in diameter) were sliced (sections of 200 μm ± 20 μm) using a Krumdieck live tissue microtome in Earle's balanced salt solution, containing 25 mmol HEPES and 17 mmol glucose. The tissue was transferred to incubation medium, additionally containing Na-Pyruvate and MEM amino acids (both Thermo Fisher Scientific), MEM vitamins and L-glutamin (both Thermo Fisher Scientific), and penicillin (100 U/mL)/streptomycin (100 μg/mL) at 37°C in the incubator. Incubation medium was changed 7 times after 30-minute wash periods and finally left overnight. Indicated treatments were started on the next day, and after 3 days, supernatants were collected and the tissue was fixed with formalin and embedded in paraffin.

Radioimmunoassay

Radioimmunoassay for the determination of PGE_2 was performed as previously described.[E9] EC_{50} of PGE_2 was 76.0 ± 7.3 pg/mL (n = 7) and detection limit, defined as 10% inhibition of binding, was at 8.5 ± 1.1 pg/mL (n = 7).

HPLC-MS/MS

Prostanoids and specialized proresolving mediators were quantified by UHPLC coupled to tandem mass spectrometry after solid-phase extraction. Prostanoids and specialized proresolving mediators were quantified by UHPLC coupled to tandem mass spectrometry after solid-phase extraction. From IPF PCLSs, 80 μL of supernatant was spiked with 20 μL of the isotopically labeled internal standards (Cayman Chemical, Ann Arbor, Mich), 200 μL PBS, 400 μL citric acid buffer (pH 5.7), and 90 μL 2,6-di-tert-butyl-4-methylphenol (BHT, 0.1% in methanol). The sample was loaded on Biotage Express ABN cartridges (Biotage, Uppsala, Sweden) and eluted with methanol (+2% ammonia solution) after washing with methanol/water (1:1; vol/vol, +2% formic acid) followed by water. Samples were evaporated to dryness in amber glass vials and reconstituted in 50 μL acetonitrile/water (2:8; vol/vol, +0.0025% formic acid).

The chromatographic separation of the analytes was carried out using an Acquity UPLC BEH C18 2.1 × 100 mm column, 1.7 μm (Waters, Eschborn, Germany) equipped with a precolumn VanGuard 2.1 × 5 mm, 1.7 μm (Waters) under gradient conditions. Water and acetonitrile, both containing 0.0025% formic acid, were used as mobile phases and sample run time was 15 minutes. The LC-MS/MS analysis was carried out using an Agilent 1290 Infinity LC system (Agilent, Waldbronn, Germany) coupled to a hybrid triple quadrupole linear ion trap mass spectrometer QTRAP 6500+ (Sciex, Darmstadt, Germany) equipped with a Turbo-V-source operating in negative electrospray ionization mode. Analysis was done in the multiple reaction monitoring mode with a dwell time of 5 ms for all analytes.

Data were acquired using Analyst Software version 1.6.2, and quantification was performed with MultiQuant Software version 3.0 (both Sciex, Darmstadt, Germany), using the internal standard method (isotope dilution mass spectrometry). The coefficient of correlation was at least 0.99. Variations in accuracy were less than 15% over the whole range of calibration, except for the lower limit of quantification, where a variation in accuracy of 20% was accepted.

Isolation and differentiation of fibrocytes

Blood was drawn from healthy volunteers according to an approved protocol by the Ethics Committee of the Medical University of Graz (17-291 ex 05/06) and PBMCs were prepared as previously described.[E10] The same procedure was followed for blood from patients with IPF (n = 9 [7 males, 2 females]; mean age, 74.5 ± 10.39 years; approved by the Ethics Committee as 30-537 ex 17/18). Informed consent was obtained before taking blood. Fibrocytes were differentiated for 5 days as described earlier in the presence of indicated treatments on chamber slides (Thermo Fisher Scientific) and stained with DiffQuick.[E11] Six photomicrographs per treatment condition were taken at 200 × magnification and counted manually in a blinded fashion.[E11] Fibrocyte counts are shown as percent of total cells.

Collagen ELISA

ELISA for the determination of Col1a1/pro-Col1a1 was done using the Duo set kit from bio-techne (Minneapolis, Minn) according to the manufacturer's instructions. Supernatants from PCLSs were used and standard curve preparation was done in the presence of medium, and values were obtained by subtracting absorption at 540 nm from that at 450 nm on a microplate reader. For calculating concentrations of collagen in supernatants, log-log standard curves were used and data were normalized to protein concentrations in the supernatants.

Image acquisition/microscopy

Fluorescence microscopy was carried out with a confocal laser scanning microscope (Zeiss LSM 510 META) and processed with ZEN software (Zeiss, Jena, Germany) and ImageJ.[E12] A UV 405 nm (DAPI), a tunable Argon 458/477/488/514 nm (AF488), and a Helium-Neon 543 nm (Cy3 and AF594) laser were used. Brightness and contrast of the photomicrographs were adjusted using ImageJ.[E13] For light microscopy, photomicrographs were acquired with an Olympus BX41 microscope with an Olympus UC90 camera and Xcellence imaging software (Olympus, Hamburg, Germany).

Data analysis

Statistical analysis was performed using GraphPad Prism 6 (GraphPad Software Inc, San Diego, Calif). For comparing 2 samples, Student *t* test or Mann-Whitney *U* test was carried out. When samples were normalized to vehicle, a 1-sample *t* test against vehicle was performed. For multiple comparisons, 1-way ANOVA followed by Tukey post hoc test for comparing all groups was performed for more than 3 groups and a Newman-Keuls post hoc test was performed in the case of 3 groups.[E14] Two-way ANOVA for repeated measurements with Bonferroni post hoc test was carried out for time courses, and Gehan-Breslow test was applied to compare survival curves. Significance was set at P less than .05. Data are given as mean ± SEM. When applicable, normality was confirmed by the Kolmogorov-Smirnov test.

REFERENCES

E1. Zhang Y, Desai A, Yang SY, Bae KB, Antczak MI, Fink SP, et al. Tissue regeneration. Inhibition of the prostaglandin-degrading enzyme 15-PGDH potentiates tissue regeneration. Science 2015;348:aaa2340.

E2. Sturm EM, Schratl P, Schuligoi R, Konya V, Sturm GJ, Lippe IT, et al. Prostaglandin E2 inhibits eosinophil trafficking through E-prostanoid 2 receptors. J Immunol 2008;181:7273-83.

E3. Frei RB, Luschnig P, Parzmair GP, Peinhaupt M, Schranz S, Fauland A, et al. Cannabinoid receptor 2 augments eosinophil responsiveness and aggravates allergen-induced pulmonary inflammation in mice. Allergy 2016;71:944-56.

E4. Vanoirbeek JA, Rinaldi M, De Vooght V, Haenen S, Bobic S, Gayan-Ramirez G, et al. Noninvasive and invasive pulmonary function in mouse models of obstructive and restrictive respiratory diseases. Am J Respir Cell Mol Biol 2010;42:96-104.

E5. Lovgren AK, Jania LA, Hartney JM, Parsons KK, Audoly LP, Fitzgerald GA, et al. COX-2-derived prostacyclin protects against bleomycin-induced pulmonary fibrosis. Am J Physiol Lung Cell Mol Physiol 2006;291:L144-56.

E6. Hubner RH, Gitter W, El Mokhtari NE, Mathiak M, Both M, Bolte H, et al. Standardized quantification of pulmonary fibrosis in histological samples. Biotechniques 2008;44:507-11, 14-7.

E7. Mikamo M, Kitagawa K, Sakai S, Uchida C, Ohhata T, Nishimoto K, et al. Inhibiting Skp2 E3 ligase suppresses bleomycin-induced pulmonary fibrosis. Int J Mol Sci 2018;19.

E8. Schlosser K, Taha M, Stewart DJ. Systematic assessment of strategies for lung-targeted delivery of microRNA mimics. Theranostics 2018;8:1213-26.

E9. Ulcar R, Peskar BA, Schuligoi R, Heinemann A, Kessler HH, Santner BI, et al. Cyclooxygenase inhibition in human monocytes increases endotoxin-induced TNF alpha without affecting cyclooxygenase-2 expression. Eur J Pharmacol 2004;501:9-17.

E10. Barnthaler T, Jandl K, Sill H, Uhl B, Schreiber Y, Grill M, et al. Imatinib stimulates prostaglandin E2 and attenuates cytokine release via EP4 receptor activation. J Allergy Clin Immunol 2019;143:794-7.e10.

E11. Pilling D, Gomer RH. Differentiation of circulating monocytes into fibroblast-like cells. Methods Mol Biol 2012;904:191-206.

E12. Pfister R, Hagemeister J, Esser S, Hellmich M, Erdmann E, Schneider CA. NT-pro-BNP for diagnostic and prognostic evaluation in patients hospitalized for syncope. Int J Cardiol 2012;155:268-72.

E13. Schneider CA, Rasband WS, Eliceiri KW. NIH Image to ImageJ: 25 years of image analysis. Nat Methods 2012;9:671-5.

E14. Seaman MA, Levin JR, Serlin RC. New developments in pairwise multiple comparisons—some powerful and practicable procedures. Psychol Bull 1991;110:577-86.

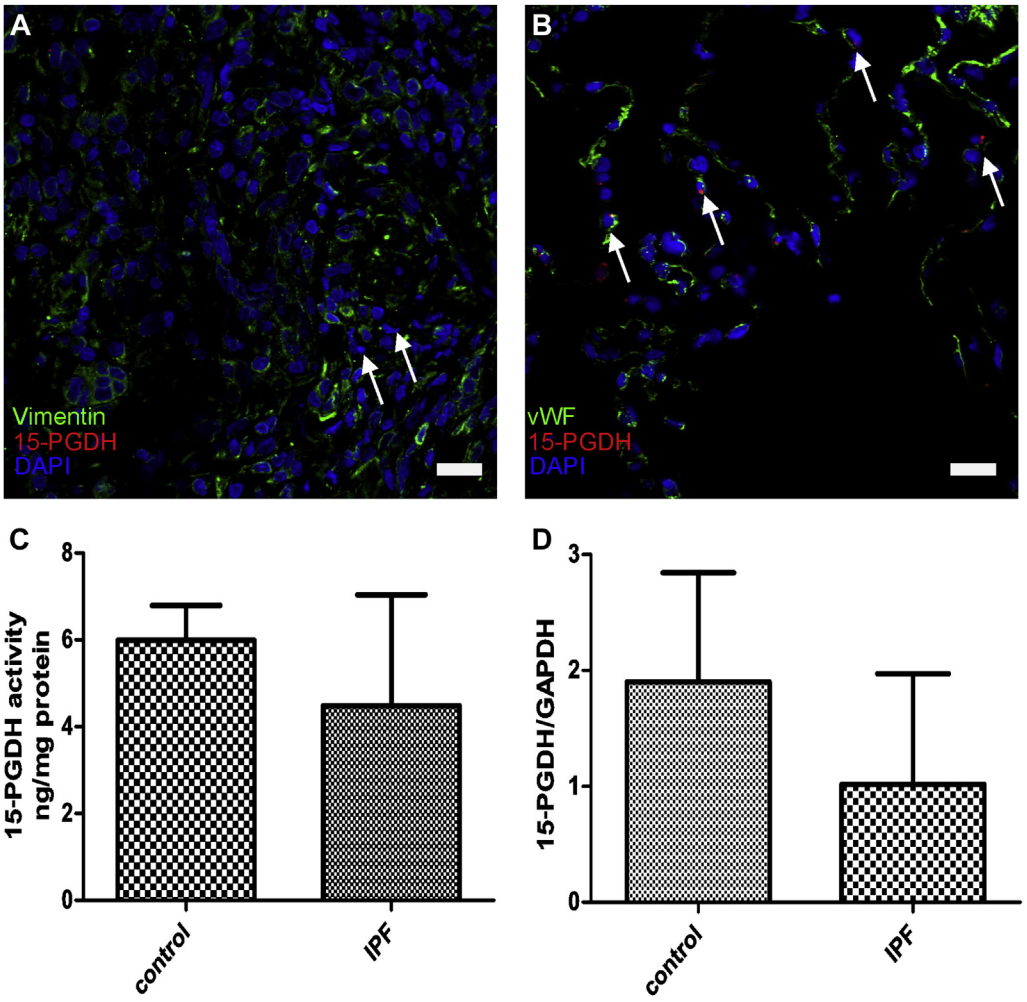

FIG E1. Vimentin-positive cells in patients with IPF show very little 15-PGDH expression, whereas vWF-positive cells are the main 15-PGDH–expressing cells in healthy lungs. 15-PGDH activity is not significantly different in patients with IPF. **A,** ISH for 15-PGDH mRNA (*red*) and immunostaining for vimentin (*green*) on IPF lungs. **B,** ISH for 15-PGDH mRNA (*red*) and immunostaining for vWF (*green*) on healthy control lungs. *Arrows* show 15-PGDH– positive cells. *Scale bars* indicate 20 μm; sections are representative for 5 controls and 5 patients with IPF. Total activity (**C**) and protein content (**D**) of 15-PGDH from whole lung lysates were not significantly different between patients with IPF and controls (n = 5, Student *t* test). *vWF*, von Willebrand factor.

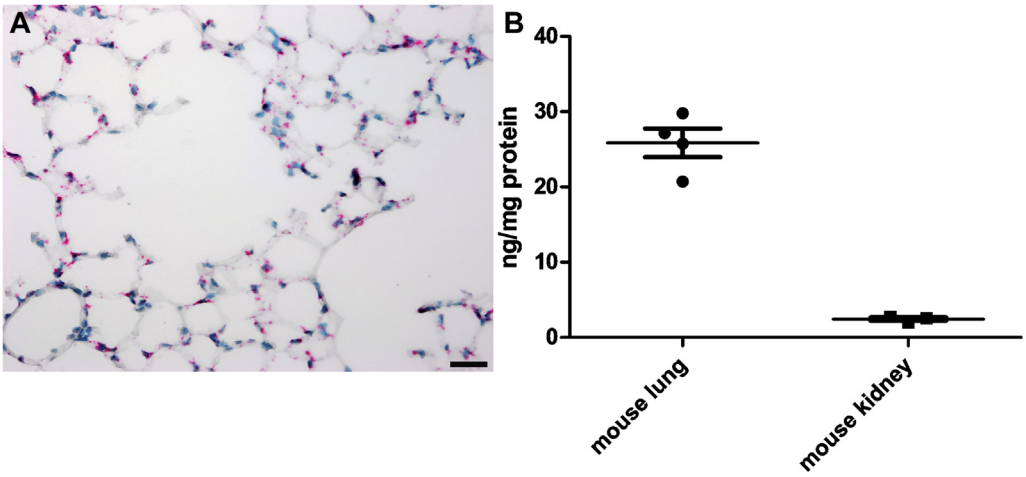

FIG E2. Mouse lungs express 15-PGDH mRNA and show considerable 15-PGDH activity. **A,** ISH for 15-PGDH mRNA (*red*) and counterstaining with methyl green on C57/Bl6 mouse lungs are representative for 5 healthy lungs. *Scale bars* indicate 20 μm. **B,** 15-PGDH activity in C57/Bl6 mouse lung as compared with kidney homogenates (n = 3-4).

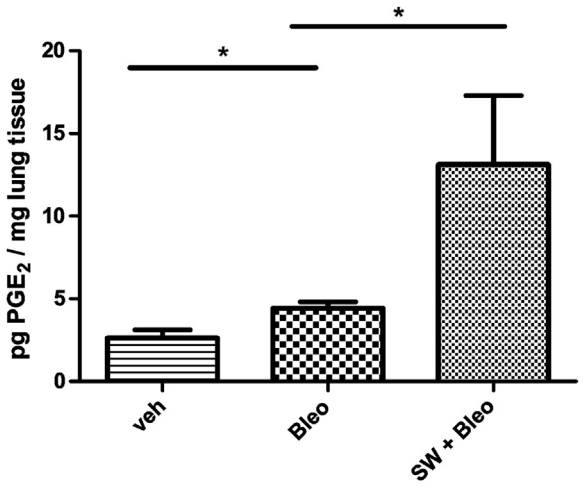

FIG E3. 15-PGDH inhibition increases PGE_2 in the lungs of bleomycine-treated mice. Pulverized lung tissue was used for mass spectrometry measurements. Mann-Whitney *U* test was performed (n = 5-10; $*P < .05$).

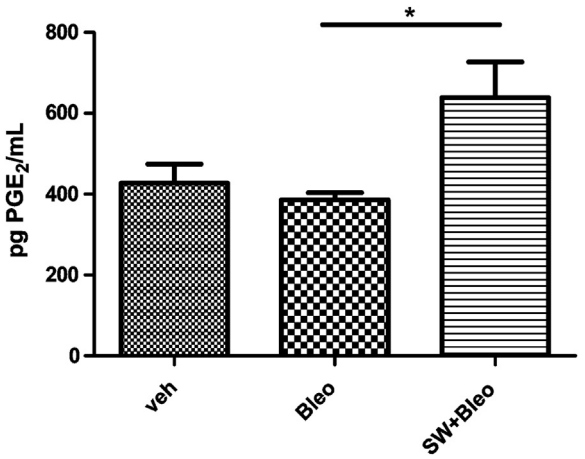

FIG E4. 15-PGDH inhibition increases PGE_2 in the bone marrow of bleomycine-treated mice. Femur was perfused with 1 mL of PBS, and PGE_2 concentration was measured by radioimmunoassay. Mann-Whitney *U* test was performed (n = 5; **P* < .05).

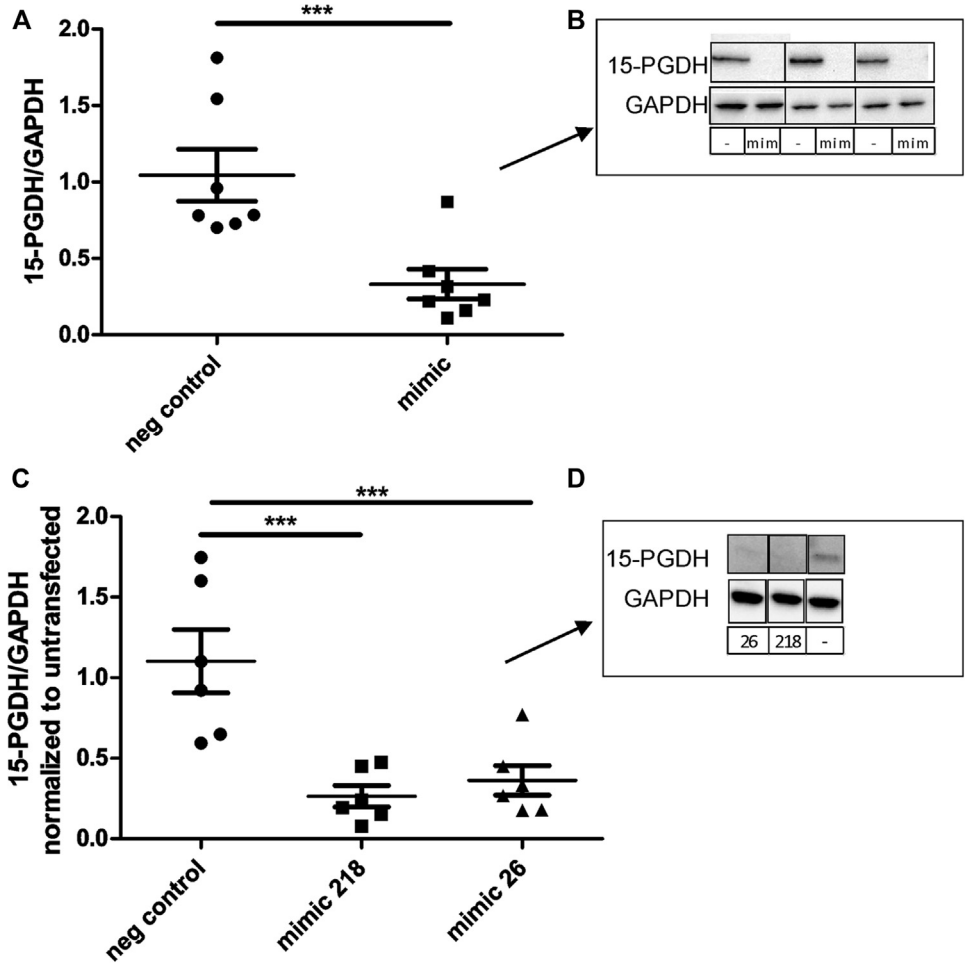

FIG E5. miRNA 26a-5p and miRNA 218-5p regulate 15-PGDH *in vitro.* A549 cells (**A**) or HK2 cells (**C**) were transfected with a mimic of (Fig E5, *C*) miRNA 218-5p (218), (Fig E5, *A*) miRNA 26a-5p (26/mimic) or a negative control (neg control/−), harvested after 72 hours and Western blot was performed. **B** and **D,** representative Western blots. (Fig E5, *A*) Statistical differences were tested by Student *t* test and (Fig E5, *C*) 1-way ANOVA, followed by Newman-Keuls *post hoc* test. ***$P < .001$.

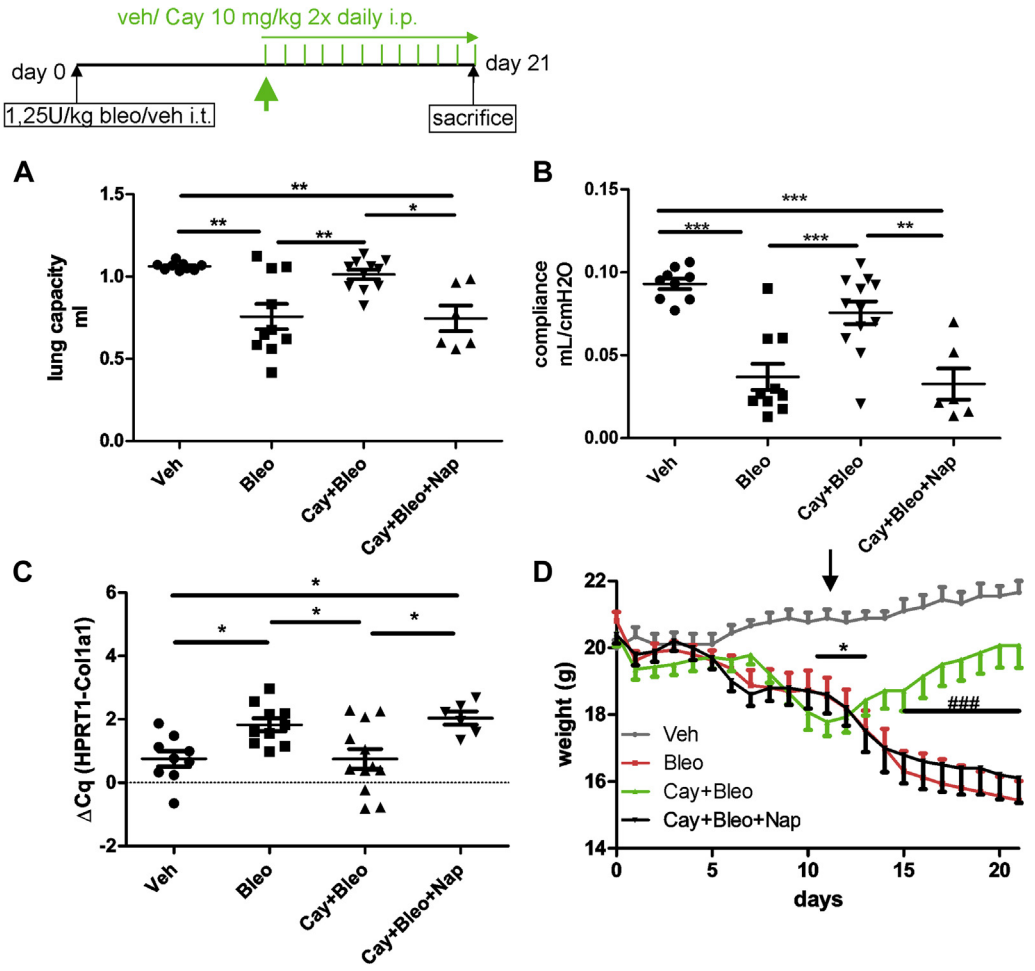

FIG E6. Inhibition of 15-PGDH by CAY10638 ameliorates bleomycin-induced pulmonary fibrosis in a therapeutic model. **A-D,** Mice were treated with vehicle (veh), bleomycin (1.25 U/kg, Bleo), 15-PGDH inhibitor plus bleomycin (Cay + Bleo; CAY10638 10 mg/kg twice daily, from day 10 onward), or 15-PGDH inhibitor plus bleomycin plus a COX inhibitor (Cay + Bleo + Nap; naproxen, 15 mg/kg, from day 10 onward). Lung capacity (**A**), compliance (**B**), and Col1a1 mRNA (**C**) were measured on day 21 and (**D**) weight was measured daily. One-way ANOVA, followed by Tukey *post hoc* test, was applied for Fig E6, *A-C* (n = 6-12). For *D*, 2-way ANOVA for repeated measurements, followed by Bonferroni post hoc test, was applied (n = 6-12). **P* < .05, ***P* < .01, ****P* < .001; in (*D*) ###*P* < .001 Cay + Bleo vs Bleo and Cay + Bleo + Nap.

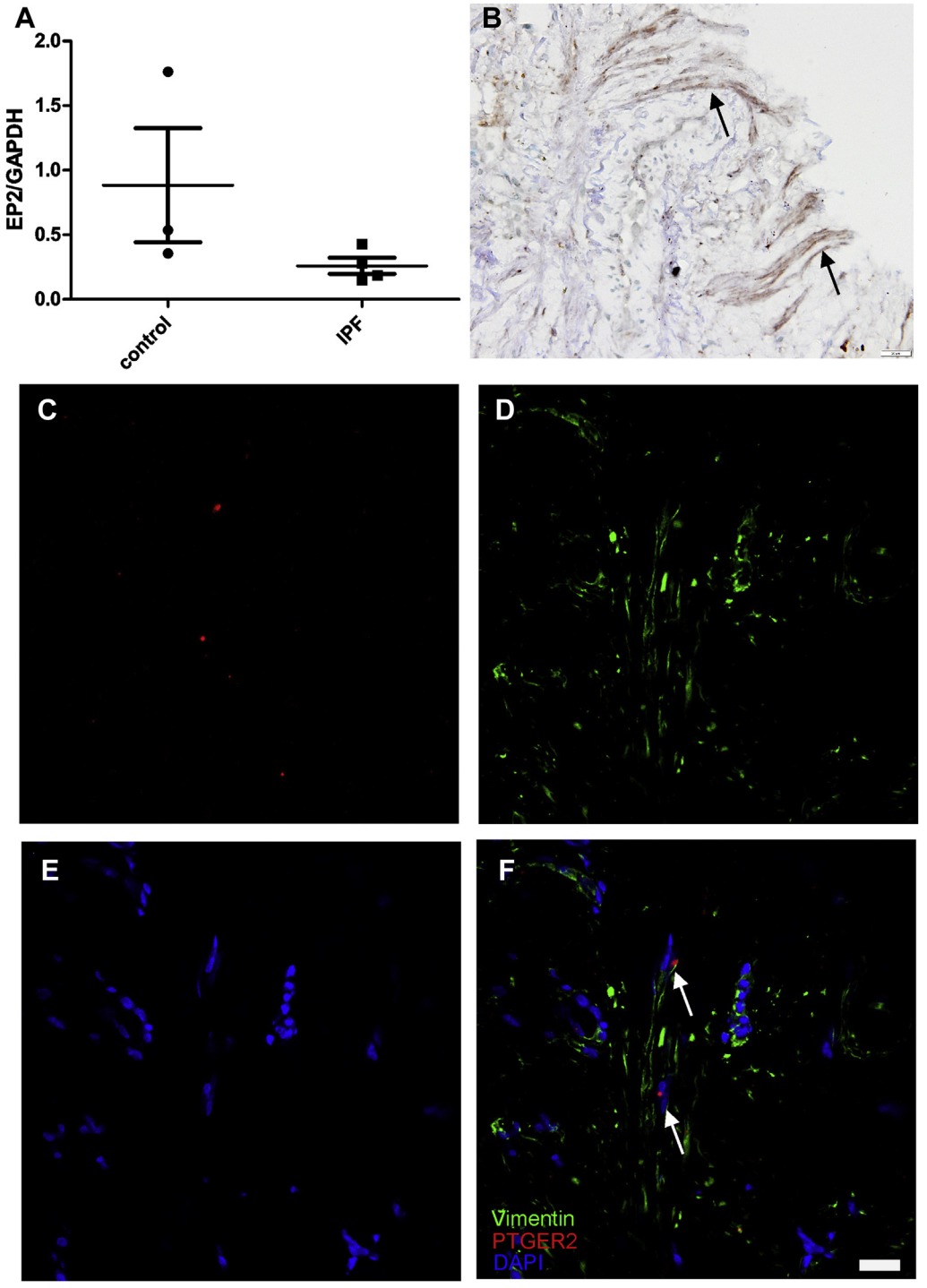

FIG E7. The EP2 receptor is expressed in PCLSs from patients with IPF. **A,** PCLSs from controls and patients with IPF (used in Fig 8) were subjected to Western blotting. **B-F,** PCLSs from patients with IPF were stained for EP2 receptor protein (Fig E7, *B*, *brown*) via immunohistochemistry and mRNA (Fig E7, *C-F*, PTGER2, *red*) via ISH. For ISH stainings, a vimentin antibody was used to detect mesenchymal cells (*green*, Fig E7, *D*), whereas *F* shows the overlay. In *A*, statistical difference was tested by Student *t* test, but no significance was detected. *Scale bar* indicates 20 μm; *white arrows* show double-positive cells, whereas *black arrows* show positive cells with spindle-shaped morphology.

TABLE E1. Antibodies used in Western blots and IF/IHC microscopy

Antibody	Host species	Company	No.	IF/IHC dilution	Western blot dilution
Primary antibody					
15-PGDH	Rabbit	Abcam	187161	1:500	—
15-PGDH	Rabbit	Abcam	178682	—	1:1000
Pro-SPC	Rabbit	Merck Millipore	AB3786	1:500	—
CD68	Mouse	Abcam	955	1:100	—
GAPDH	Rabbit	Cell Signaling	2118S	—	1:5000
VE-cadherin	Mouse	Santa Cruz	sc-9989	1:200	—
α-SMA	Rabbit	Abcam	5694	1:1000	—
Vimentin	Rat	R and D Systems	MAB2105	1:100	—
vWF	Rabbit	Dako	A0082	1:500	—
Cleaved caspase 3	Rabbit	Gentaur	MAB835-SP	1:50	—
Ki-67	Rabbit	Cell Signaling	12202S	1:100	—
FSP	Rabbit	Merck Millipore	07-2274	1:500	—
EP2	Rabbit	Cayman	101750	1:100	1:1000
CD45	Rat	Sigma	SAB4700578	1:100	—
Secondary antibody					
Anti-rabbit Cy3	Goat	Invitrogen	A-10520	1:500	—
Anti-rabbit AF488	Goat	Invitrogen	A-11008	1:500	—
Anti-rabbit AF647	Goat	Invitrogen	A-21244	1:500	—
Anti-rat AF647	Goat	Invitrogen	A-21247	1:500	—
Anti-rat AF488	Goat	Invitrogen	A-11006	1:500	—
Anti-mouse AF488	Goat	Invitrogen	A-11001	1:500	—
Anti-rabbit HRP	Goat	Cell Signaling	70745	—	1:10000

α-SMA, α-Smooth muscle actin; *IF*, immunofluorescence; *IHC*, immunohistochemistry; *VE-cadherin*, vascular endothelial cadherin; *vWF*, von Willebrand factor.